Experimental Aspects of Polarization Observables in ep→ep at Large Momentum Transfer

Andrew Puckett

Jefferson Lab

Experimental and theoretical aspects of the proton form factors

St.Petersburg, Gatchina,

Petersburg Nuclear Physics Institute (PNPI), July 9 - 11, 2012

Outline

- Introduction: Born Approximation for ep→ep
- Polarization transfer method
- Cross-section/polarization discrepancy and the GEp crisis
- The GEp-III and GEp-2γ experiments in Hall C
  - Kinematics
  - Experiment Apparatus
  - Data Analysis
  - Results
- Re-analysis of GEp-II data (Hall A)
- Future prospects at JLab
  - New recoil polarization measurements
  - Polarized target measurements
  - A_N in ep→ep

ep→ep in the Born Approximation

$$
\begin{aligned}
\mathcal{J}^{\mu}(0) &= \bar{u}(P')\left[F_1(Q^2)\gamma^{\mu} + F_2(Q^2)\frac{i\sigma^{\mu\nu}q_{\nu}}{2M}\right]u(P) \\
G_E &= F_1 - \tau F_2 \\
G_M &= F_1 + F_2 \\
\frac{d\sigma}{d\Omega_e} &= \frac{\alpha^2}{Q^2}\left(\frac{E'}{E}\right)^2\left[\frac{G_E^2+\tau G_M^2}{1+\tau}\cot^2\frac{\theta_e}{2} + 2\tau G_M^2\right] \\
&= \left(\frac{d\sigma}{d\Omega_e}\right)_{Mott} \times \frac{\epsilon G_E^2+\tau G_M^2}{\epsilon(1+\tau)} \\
\tau &= \frac{Q^2}{4M^2}, \epsilon = \left(1+2(1+\tau)\tan^2\frac{\theta_e}{2}\right)^{-1}
\end{aligned}
$$

$$
\begin{aligned}
P_t &= -\sqrt{\frac{2\epsilon(1-\epsilon)}{\tau}}\frac{r}{1+\frac{\epsilon}{\tau}r^2} \\
P_\ell &= \frac{\sqrt{1-\epsilon^2}}{1+\frac{\epsilon}{\tau}r^2} \\
r \equiv \frac{G_E}{G_M} &= -\frac{P_t}{P_\ell}\sqrt{\frac{\tau(1+\epsilon)}{2\epsilon}} \equiv \frac{R}{\mu} \\
A &= -\frac{1}{1+\frac{\epsilon}{\tau}r^2}\left[\sqrt{\frac{2\epsilon(1-\epsilon)}{\tau}}\sin\theta^*\cos\phi^* r + \right. \\
&\left. \sqrt{1-\epsilon^2}\cos\theta^*\right]
\end{aligned}
$$

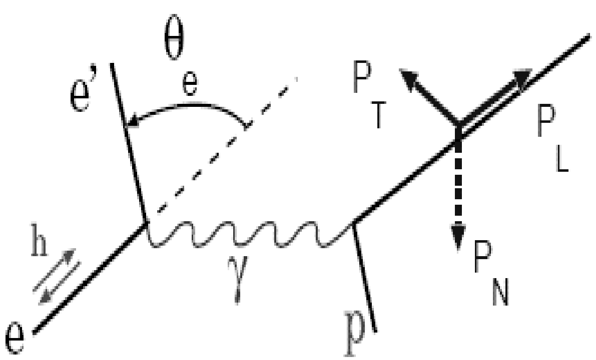

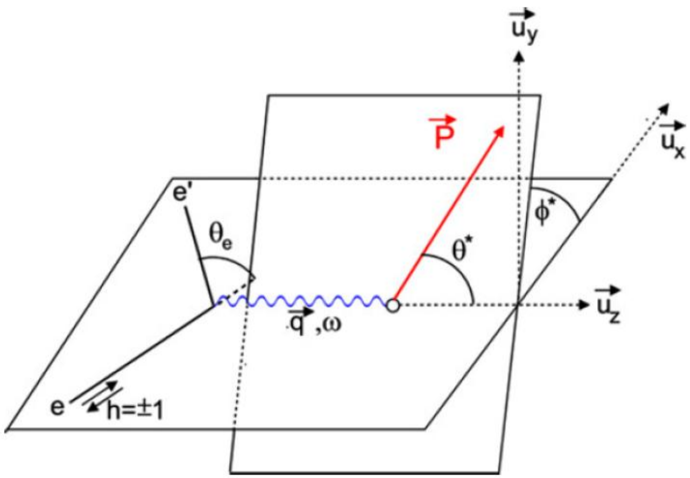

Polarization Transfer Method

- Measure the transferred polarization to the recoil proton in the scattering of longitudinally polarized electrons on unpolarized protons
  - Transferred polarization has longitudinal and transverse components parallel to the reaction plane
  - Normal component is zero
- Ratio of polarization components is directly proportional to ratio of form factors, G_E/G_M.
  - Original motivation: enhanced sensitivity to G_E at large Q^2 (relative to Rosenbluth, for which G_E sensitivity vanishes as $Q^2 \rightarrow \infty$).
  - Experimentally robust: most systematic errors cancel in the ratio or with fast beam helicity flip

The G_{Ep} "Crisis"

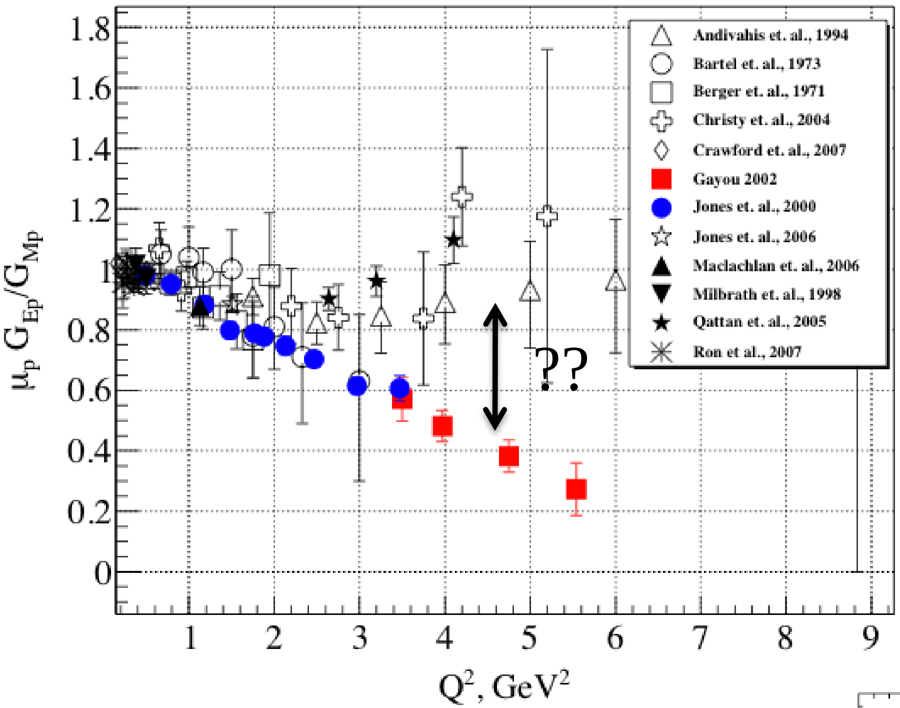

Guichon and Vanderhaeghen, PRL 91, 142303 (2003): "This discrepancy is a serious problem as it generates confusion and doubt about the whole methodology of lepton scattering experiments."

- Shockingly, polarization data of unprecedented precision completely inconsistent with existing x. sec. data!

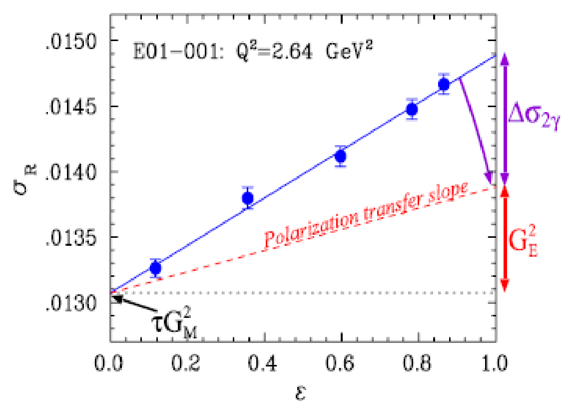

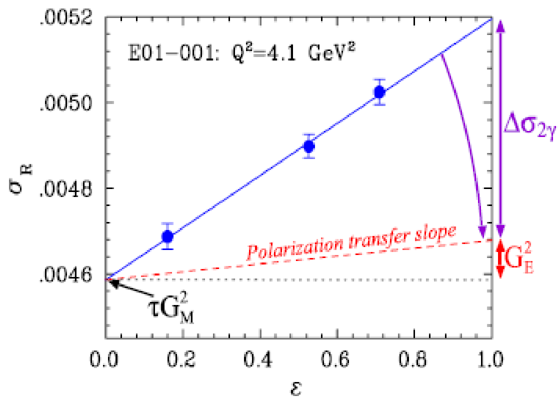

Why the PT data are more reliable

- The plot at right shows the *maximum* fractional contribution of the G_E^2 term to the reduced Born cross section vs. Q^2
- Sensitivity of the ***Born*** cross section to G_E becomes comparable to, or smaller than, the sensitivity of the ***measured*** cross section to higher-order effects that grow with Q^2
- PT ratio is directly proportional to G_E/G_M at any Q^2, and thus more robust against higher-order QED effects

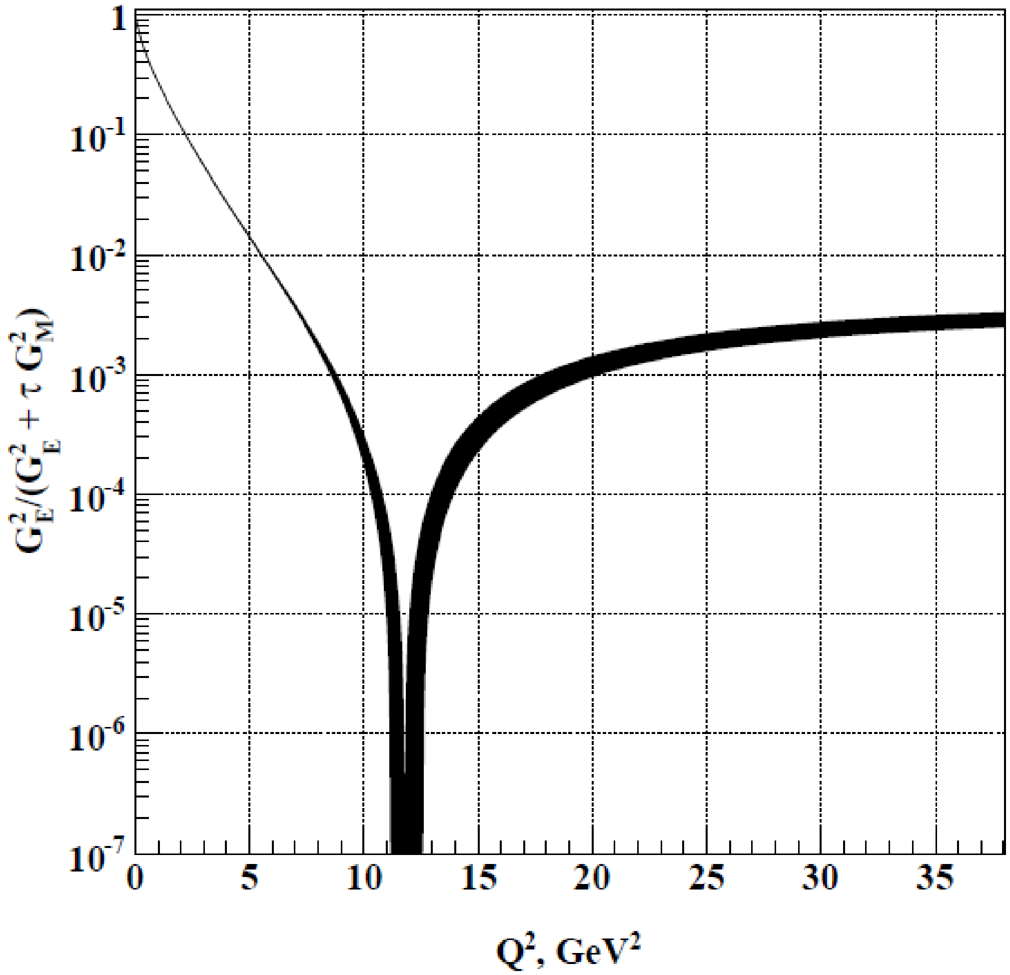

Design Considerations for PT Experiments

$$\text{At large } Q^2, \frac{d\sigma}{d\Omega} \rightarrow \frac{4\alpha^2 E^2}{Q^4}\left(\frac{E'}{E}\right)^3 \frac{G_M^2}{\epsilon} \propto \frac{E^2}{Q^{12}}$$

$$A_y \propto \frac{1}{p_p} \propto \frac{M}{Q^2}$$

$$\text{Statistical FOM} \propto N A_y^2 \propto \frac{E^2}{Q^{16}}$$

$$P_t \propto \sqrt{2\epsilon(1-\epsilon)}$$

- Naive figure-of-merit for a given E, Q^2 scales as E^2/Q^{16}
- For a given Q^2, higher E → higher count rate
- Energy dependence of P_t at fixed Q^2 leads to an optimal FOM at $\varepsilon \sim 0.5$, or typically $\theta_e \sim 45^\circ$.
- Coincident detection of scattered electron is usually required to suppress backgrounds at large Q^2
    - In a coincidence measurement, acceptance-matching is critical!

Jefferson Lab

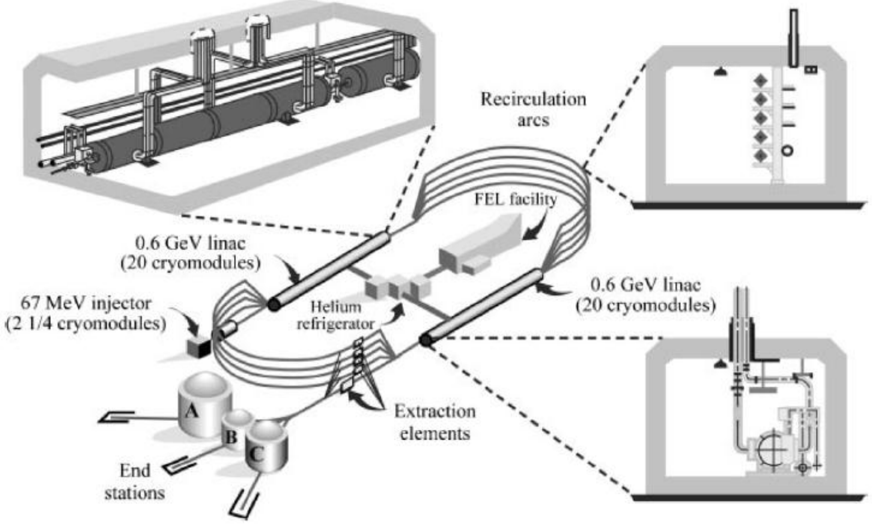

Figure 3-1: Schematic of the CEBAF accelerator

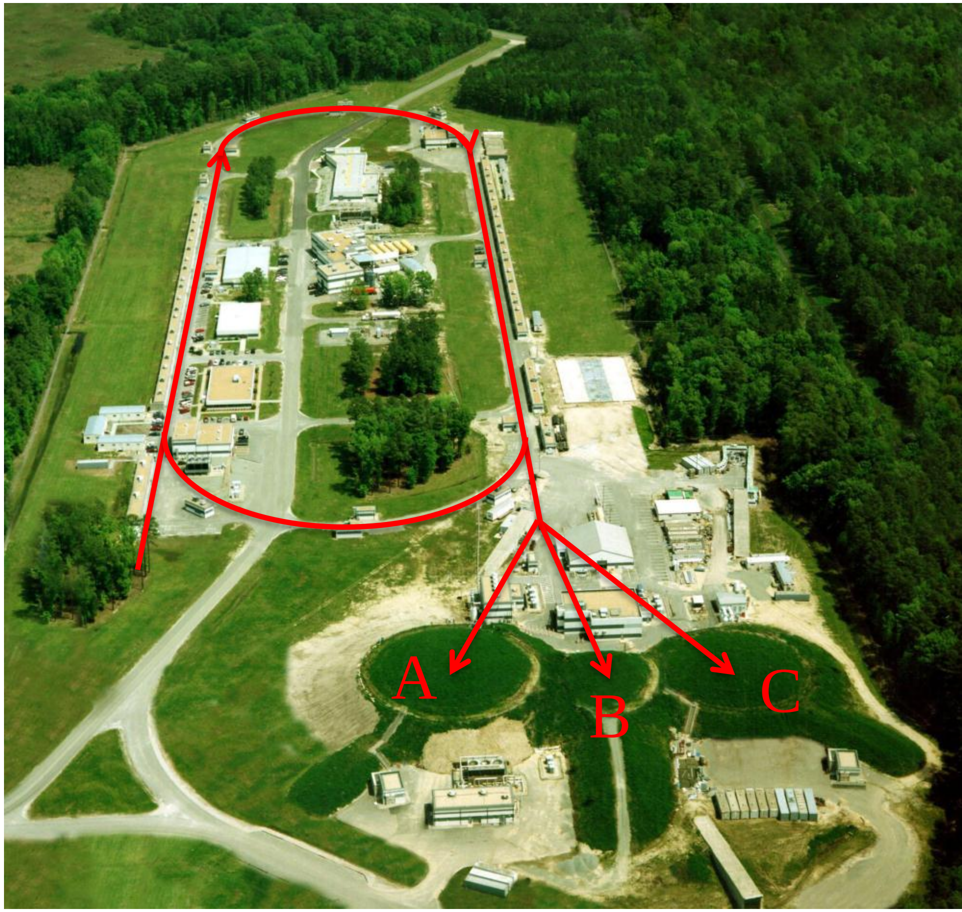

JLab Site Aerial

- CW, recirculating linac, up to 6 GeV, ~85% polarized, 100 μA
- Upgrade to 12 GeV in progress

Jefferson Lab

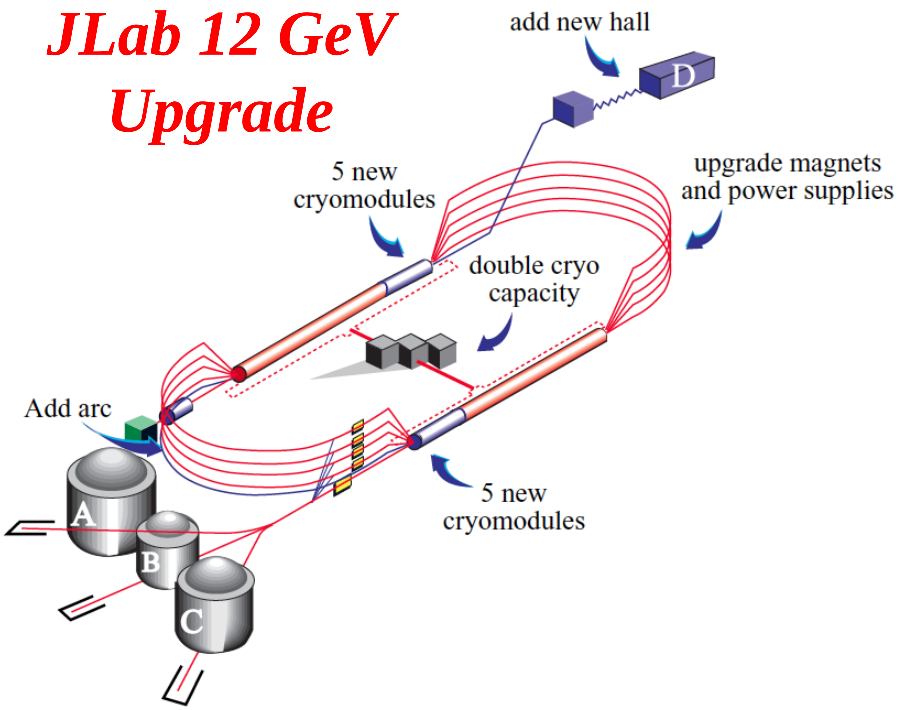

- CW, recirculating linac, up to 6 GeV, ~85% polarized, 100 μA
- Upgrade to 12 GeV in progress

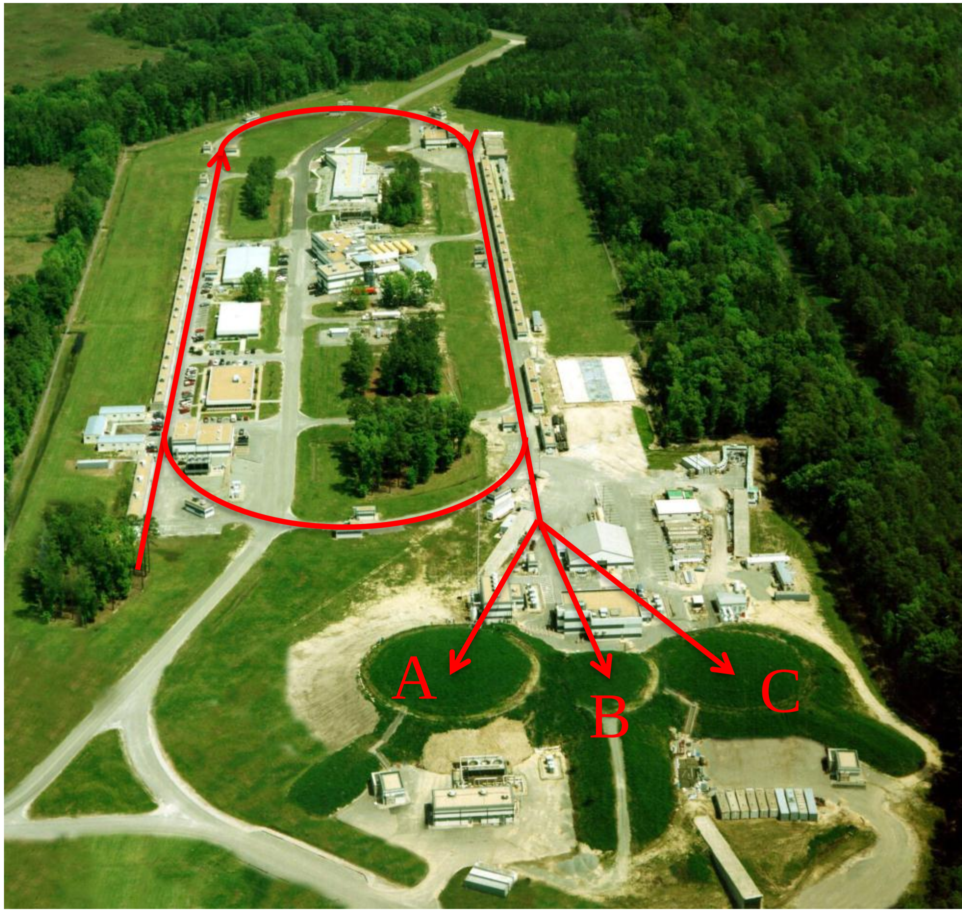

JLab Site Aerial

The GEp-III and GEp-2γ Experiments

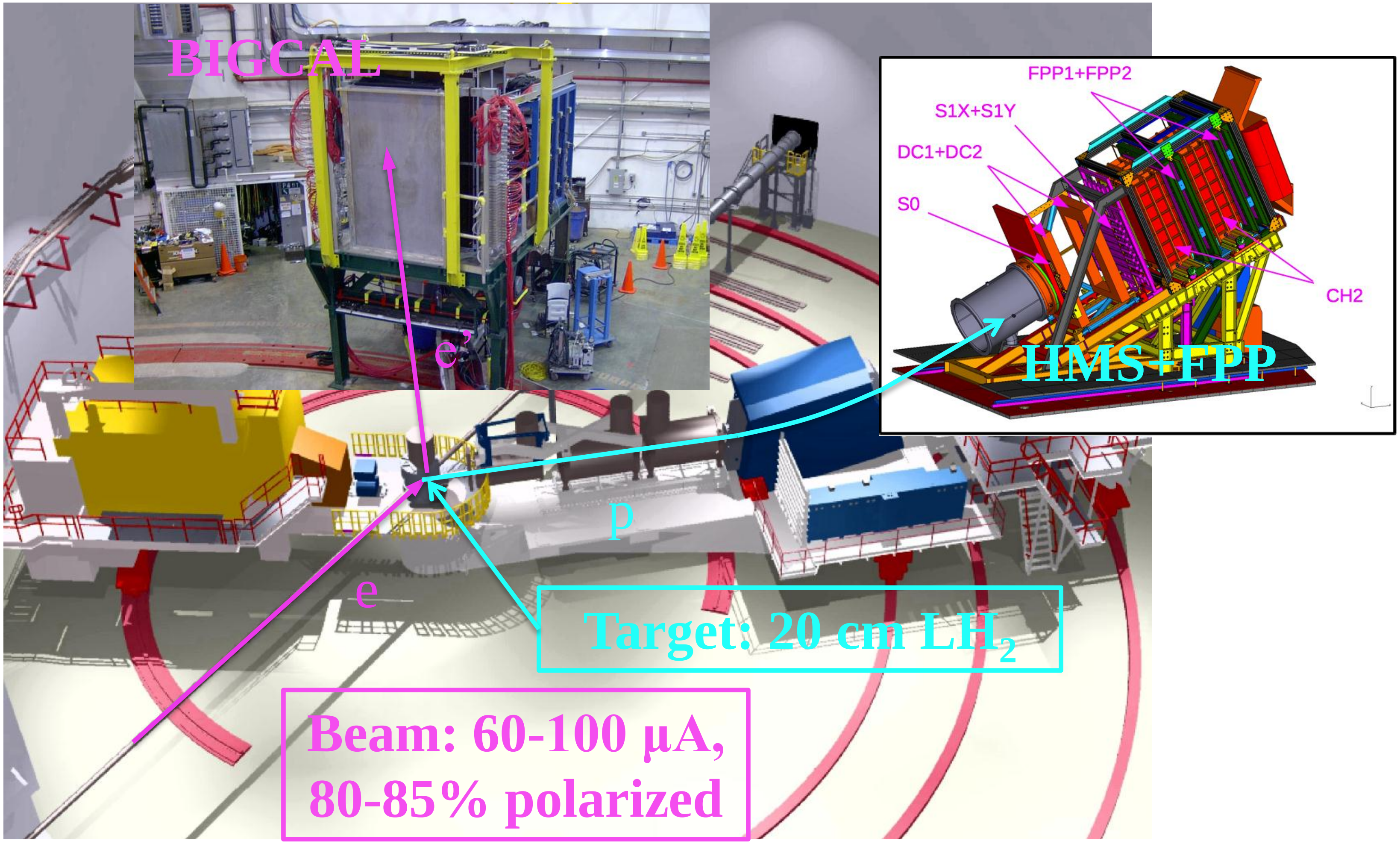

Polarization Transfer in ^{1}H(**e**,e'**p**):

Nominal *ep* luminosity ~4×10^{38} Hz/cm^2

The GEp-III/GEp-2γ Collaboration

Recoil Polarization Measurements of the Proton Electromagnetic Form Factor Ratio to $Q^2 = 8.5$ GeV^2

A. J. R. Puckett,[1,*] E. J. Brash,[2,3] M. K. Jones,[3] W. Luo,[4] M. Meziane,[5] L. Pentchev,[5] C. F. Perdrisat,[5] V. Punjabi,[6] F. R. Wesselmann,[6] A. Ahmidouch,[7] I. Albayrak,[8] K. A. Aniol,[9] J. Arrington,[10] A. Asaturyan,[11] H. Baghdasaryan,[12] F. Benmokhtar,[13] W. Bertozzi,[1] L. Bimbot,[14] P. Bosted,[3] W. Boeglin,[15] C. Butuceanu,[16] P. Carter,[2] S. Chernenko,[17] E. Christy,[8] M. Commisso,[12] J. C. Cornejo,[9] S. Covrig,[3] S. Danagoulian,[7] A. Daniel,[18] A. Davidenko,[19] D. Day,[12] S. Dhamija,[15] D. Dutta,[20] R. Ent,[3] S. Frullani,[21] H. Fenker,[3] E. Frlez,[12] F. Garibaldi,[21] D. Gaskell,[3] S. Gilad,[1] R. Gilman,[3,22] Y. Goncharenko,[19] K. Hafidi,[10] D. Hamilton,[23] D. W. Higinbotham,[3] W. Hinton,[6] T. Horn,[3] B. Hu,[4] J. Huang,[1] G. M. Huber,[16] E. Jensen,[2] C. Keppel,[8] M. Khandaker,[6] P. King,[18] D. Kirillov,[17] M. Kohl,[8] V. Kravtsov,[19] G. Kumbartzki,[22] Y. Li,[8] V. Mamyan,[12] D. J. Margaziotis,[9] A. Marsh,[2] Y. Matulenko,[19] J. Maxwell,[12] G. Mbianda,[24] D. Meekins,[3] Y. Melnik,[19] J. Miller,[25] A. Mkrtchyan,[11] H. Mkrtchyan,[11] B. Moffit,[1] O. Moreno,[9] J. Mulholland,[12] A. Narayan,[20] S. Nedev,[26] Nuruzzaman,[20] E. Piasetzky,[27] W. Pierce,[2] N. M. Piskunov,[17] Y. Prok,[2] R. D. Ransome,[22] D. S. Razin,[17] P. Reimer,[10] J. Reinhold,[15] O. Rondon,[12] M. Shabestari,[12] A. Shahinyan,[11] K. Shestermanov,[19,†] S. Širca,[28] I. Sitnik,[17] L. Smykov,[17,†] G. Smith,[3] L. Solovyev,[19] P. Solvignon,[10] R. Subedi,[12] E. Tomasi-Gustafsson,[14,29] A. Vasiliev,[19] M. Veilleux,[2] B. B. Wojtsekhowski,[3] S. Wood,[3] Z. Ye,[8] Y. Zanevsky,[17] X. Zhang,[4] Y. Zhang,[4] X. Zheng,[12] and L. Zhu[1]

The GEp-III/GEp-2γ Collaboration

Recoi … Ratio

A. J. … t,[5] V.
Punja … ,[11] H.
Bagh … ,[16] P.
Carter,[2] … iel,[18] A.
Daviden … ldi,[21] D.
Gask … [3] W.
Hinto … ,[18] D.
Kirill … arsh,[2]
Y. … H.
Mkrtchy … etzky,[27]
W. … O.
Ronc … † G.
Smit … ux,[2]
B. F … hu[1]

GEp-III/2γ Kinematics

Q^2, GeV^2	ε	E_{beam}, GeV	θ_p, °	p_p, GeV	E_e, GeV	θ_e,°
2.5	0.154	1.873	14.495	2.0676	0.532	105.2
2.5	0.633	2.847	30.985	2.0676	1.51	44.9
2.5	0.789	3.680	36.10	2.0676	2.37	30.8
5.2	0.377	4.053	17.94	3.5887	1.27	60.3
6.8	0.507	5.714	19.10	4.4644	2.10	44.2
8.5	0.236	5.714	11.6	5.407	1.16	69.0

- GEp-2γ: High-precision measurements of ε-dependence of PT ratio at $Q^2 = 2.5$ GeV^2
- GEp-III: Three new measurements at high Q^2
- Collected data from Oct. 2007-June 2008 in Hall C at JLab.

High Momentum Spectrometer (HMS)

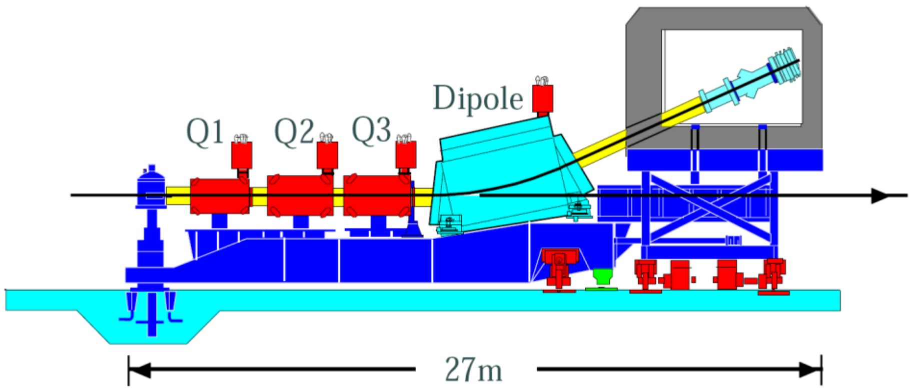

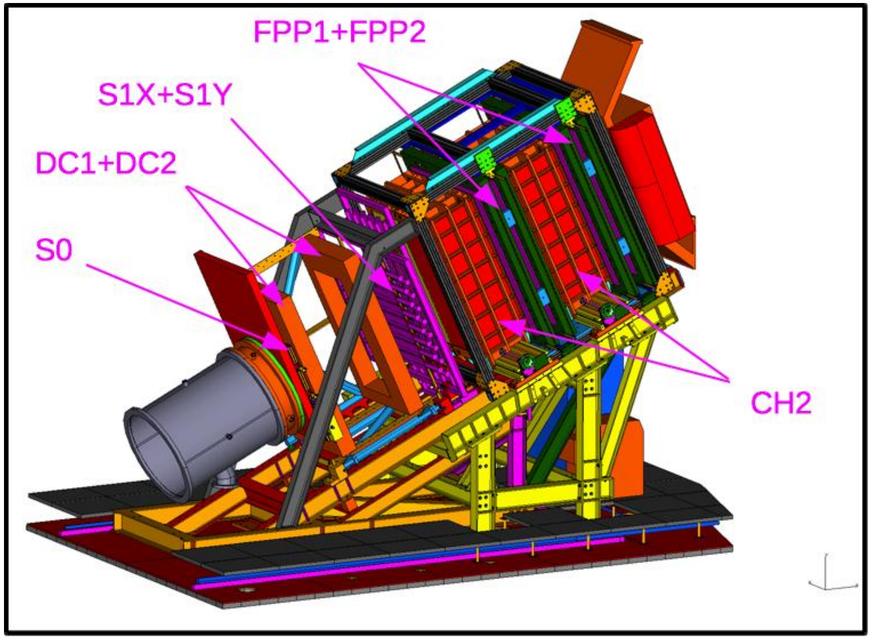

- QQQD superconducting, 25° vertical bend magnetic spectrometer
- Acceptance:
  - 6.74 msr solid angle (~2:1 vertical/horizontal aspect ratio)
  - ±9% momentum bite
  - ±5 cm/sin ϑ extended target acceptance
- Resolution:
  - $\delta p/p \sim 0.1\%$
  - Angular resolution ~1 mrad
  - Vertex resolution ~2 mm

Detector package for GEp-III

- Drift chambers: track scattered protons for kinematics reconstruction and incident FPP track definition
- Scintillator hodoscopes: trigger and timing (resolution ~250 ps)
- FPP: measure proton polarization

Hall C Focal Plane Polarimeter (FPP)

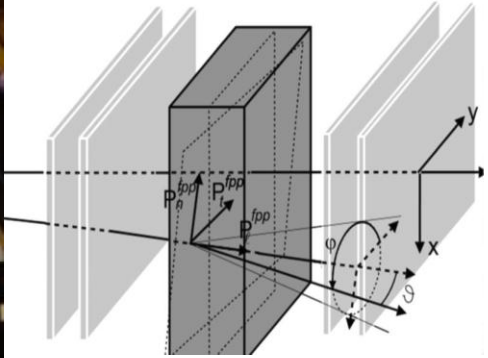

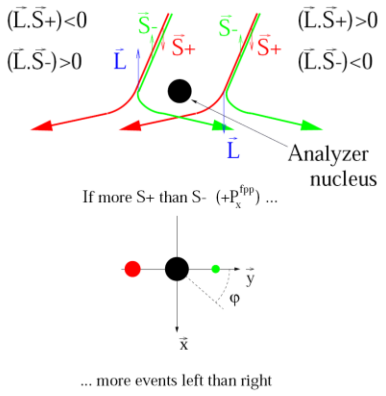

$$N^{\pm}(p,\vartheta,\varphi) = N_0^{\pm}\frac{\varepsilon(p,\vartheta)}{2\pi}\Big[1 + \big(\pm A_y P_x^{\mathrm{FPP}} + c_1\big)\cos\varphi + \big(\mp A_y P_y^{\mathrm{FPP}} + s_1\big)\sin\varphi + c_2\cos(2\varphi) + s_2\sin(2\varphi) + \cdots\Big], \qquad (4)$$

- The FPP after installation in Hall C in 2007
- Dual role of HMS drift chambers:
  - Measure kinematics of the scattered proton in ep→ep
  - Define the “beam” for the secondary scattering in CH_2

- Proton polarimetry based on spin-orbit coupling in **p**+CH_2 scattering
- Double FPP provides ~50% efficiency gain relative to single polarimeter of equivalent thickness.

FPP Angular Distributions in GEp-III/2γ

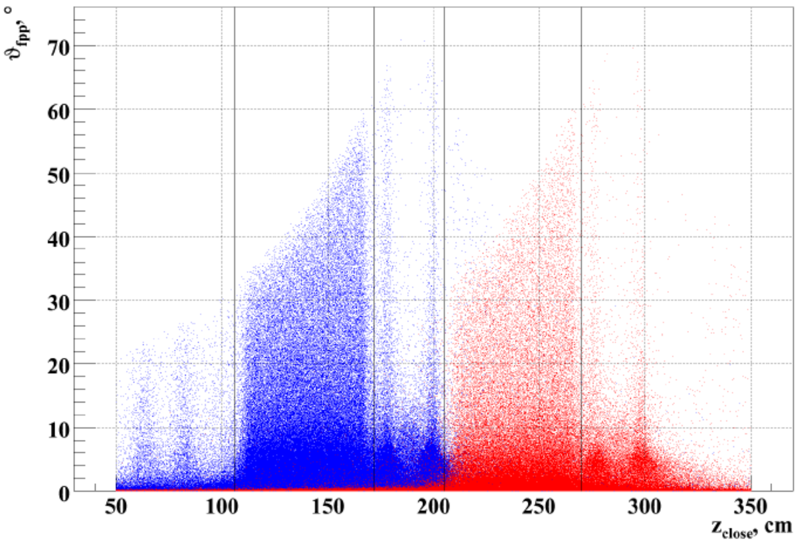

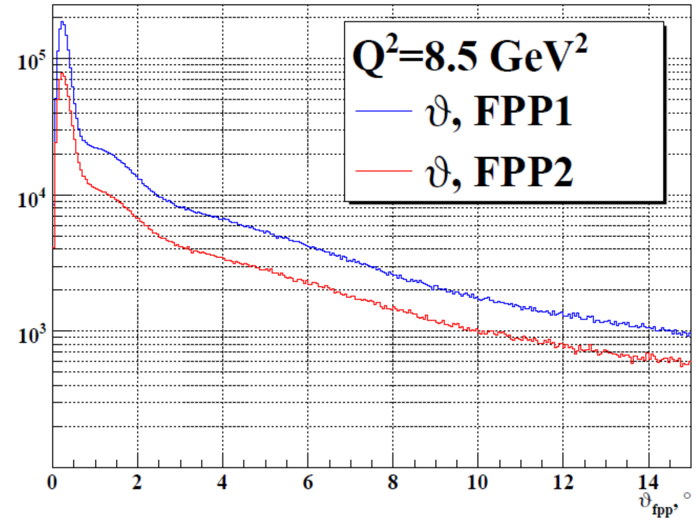

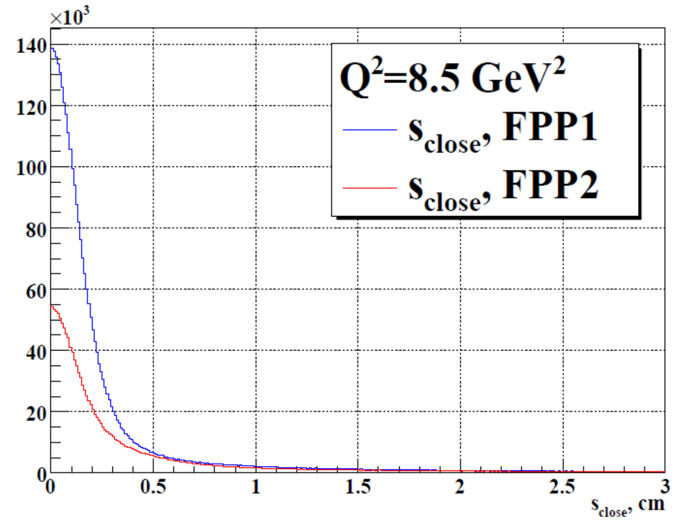

- Correlation between scattering vertex and scattering angle for events passing "cone test":
  - ***Full geometric acceptance for scattering angles up to 30-60 deg. (z-dependent)***

FPP Tracking Performance—Resolution

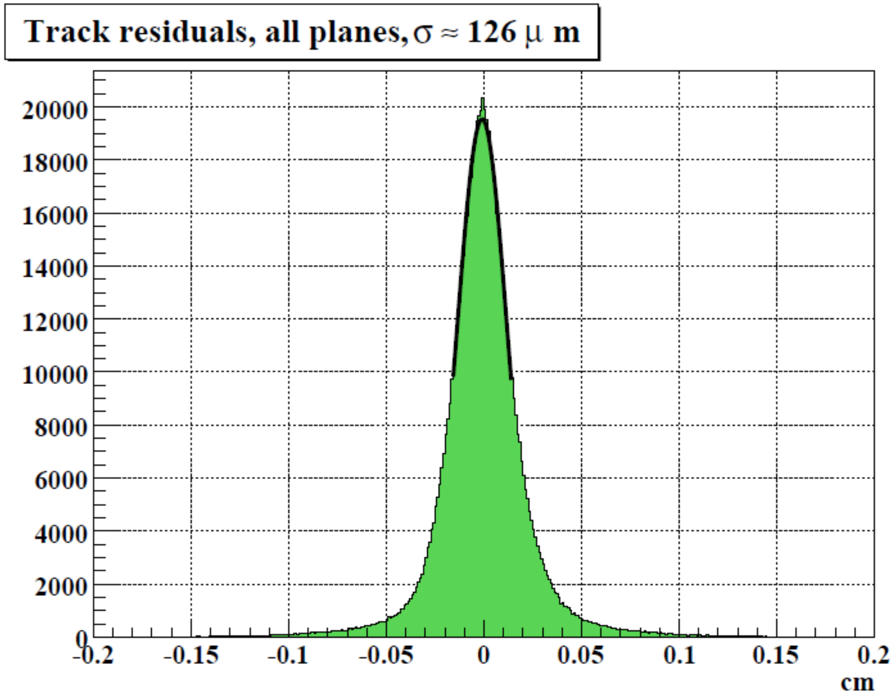

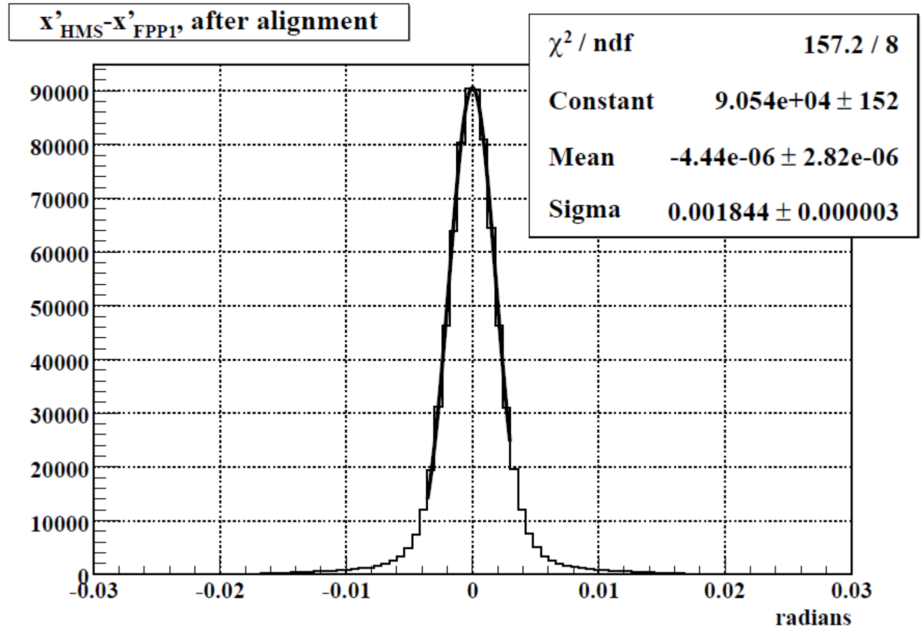

- 100-200 μm coordinate resolution → 1-2 mrad angular resolution (momentum-dependent due to multiple-scattering contribution
- "Straight-through" data with analyzers removed were obtained to provide for software alignment of the FPP drift chambers

BigCal—Electromagnetic Calorimeter

BigCal in Hall C, 2007

- TF1 lead-glass, 1744 bars, ~4×4×40 cm^3.
- Russian FEU84 PMTs
- 4" Aluminum absorber in front to mitigate rad. damage

- At large Q^2 and fixed E, Jacobian in elastic ep scattering grows large
- At $Q^2 = 8.5$ GeV^2, $\Delta\Omega_e/\Delta\Omega_p$ grows large (~140)
- To match the proton acceptance (fixed by HMS), a large-acceptance electron arm is needed
- Lead-glass calorimeter is a natural solution
  - Efficient trigger for electrons with threshold of ~ ½ ep elastic energy→reduce DAQ rate
  - Excellent coordinate/angular resolution for offline elastic event selection via angular correlations

BigCal Performance in GEp-III

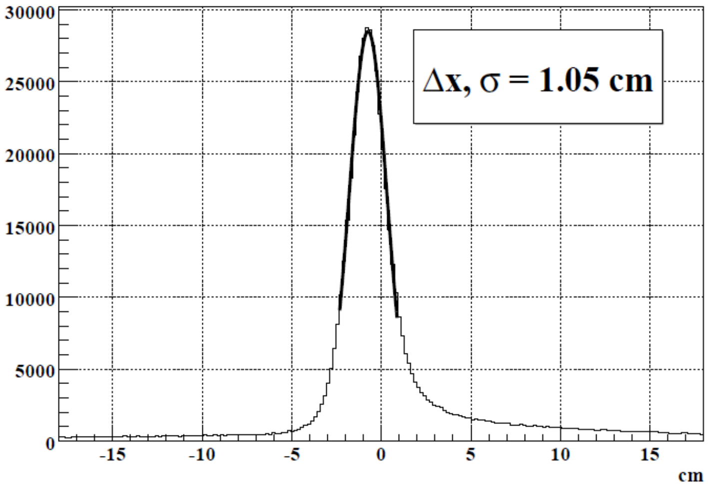

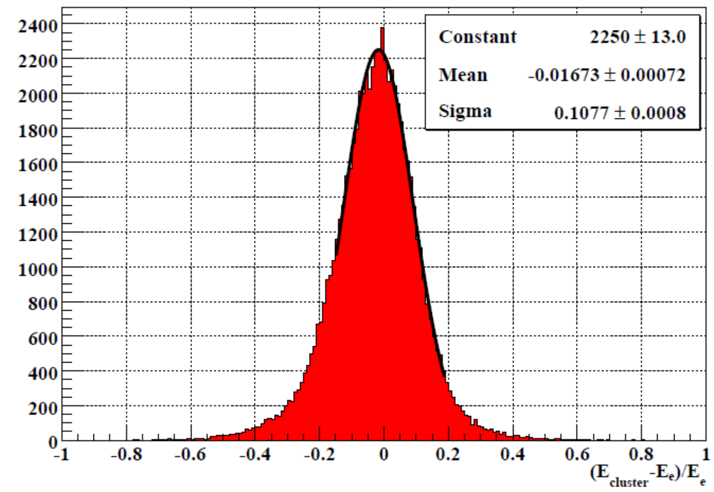

- Top left: BigCal coordinate resolution ~6 mm @2.1 GeV (after subtracting proton arm contribution)
- Top right: BigCal energy resolution ~10%/√E after two beam-weeks (with 4” Al absorber)
- Bottom right: BigCal timing resolution ~1.5 ns

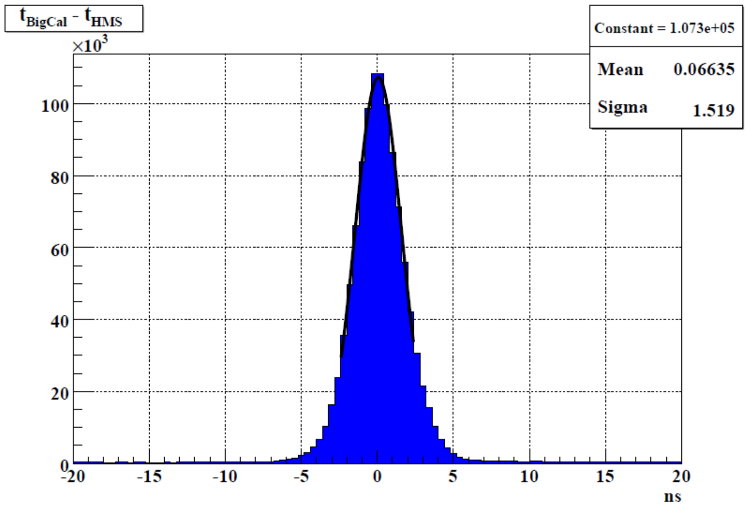

Data Analysis—Elastic Event Selection

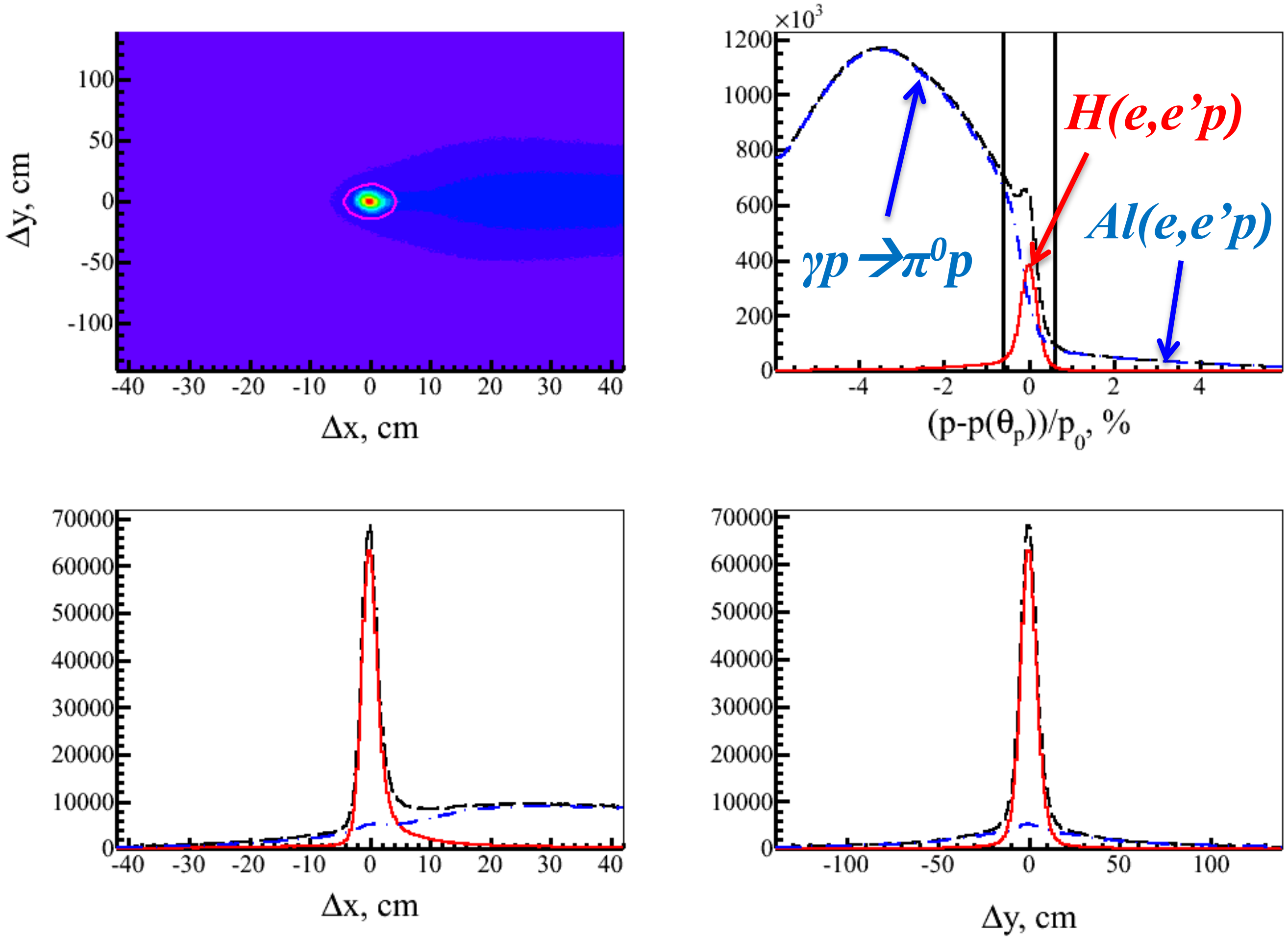

Elastic event selection, $Q^2 = 8.5\ GeV^2$

- Cuts applied to three kinematic correlations to select elastic events:

1. Electron polar angle vs. proton momentum (Δx)
2. Coplanarity (Δy)
3. Proton angle vs. proton momentum

Data Analysis—Background Subtraction

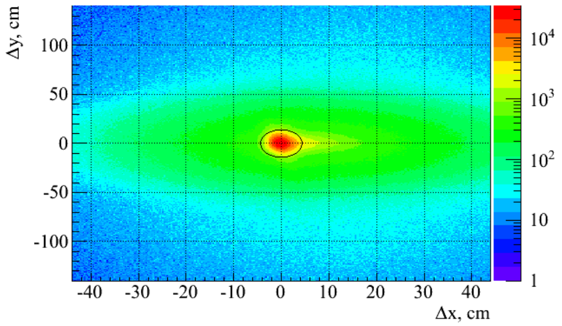

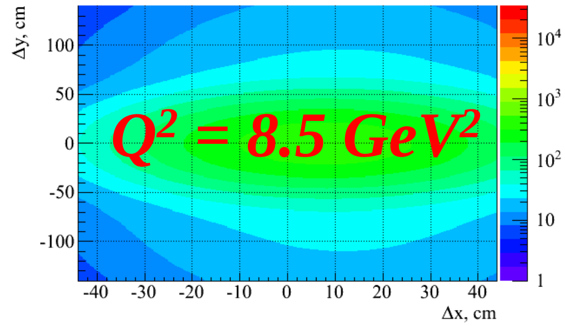

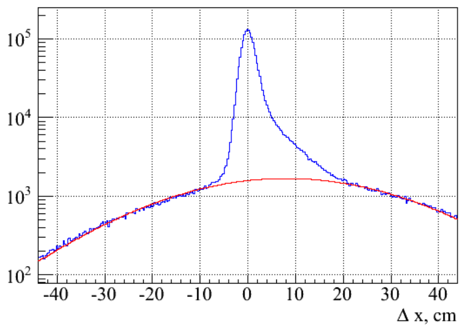

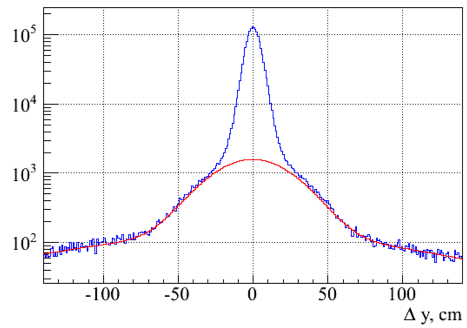

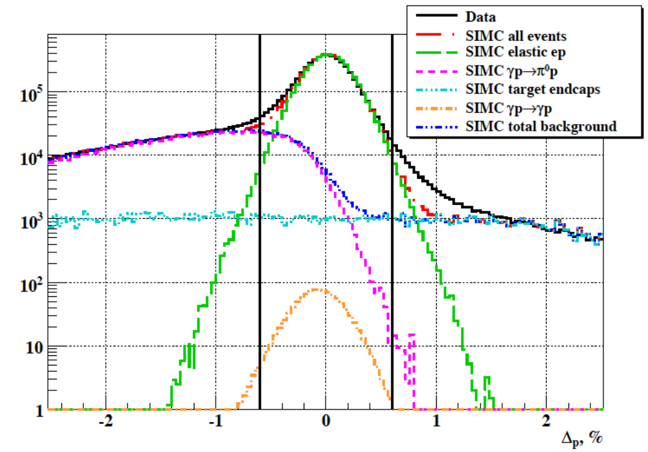

- Above: Monte Carlo calculation of signal/backgrounds
- Below: Stability of background-subtracted R wrt cut variations

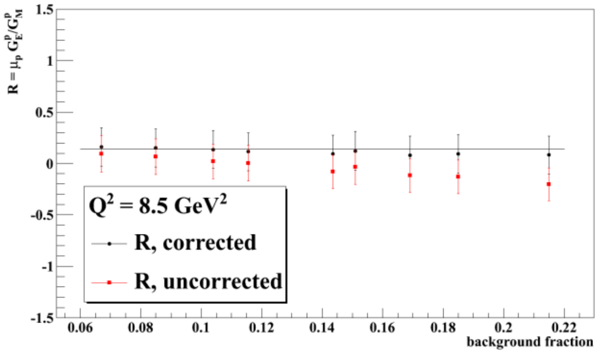

- Fits to 2D shape of background distribution in Δx, Δy plot
- Fit method agrees with Monte Carlo calculations (top right)

Analysis—Focal Plane Asymmetry

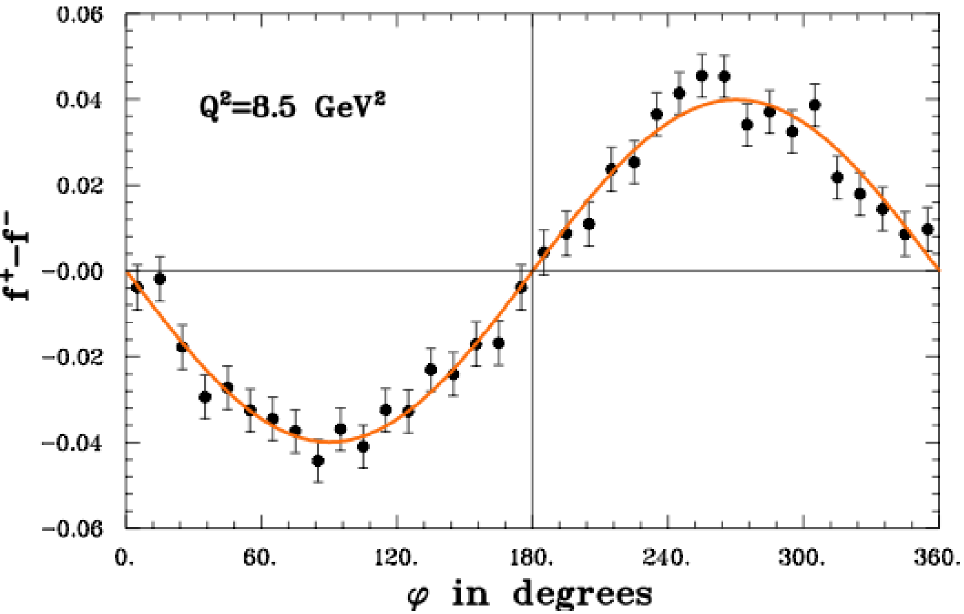

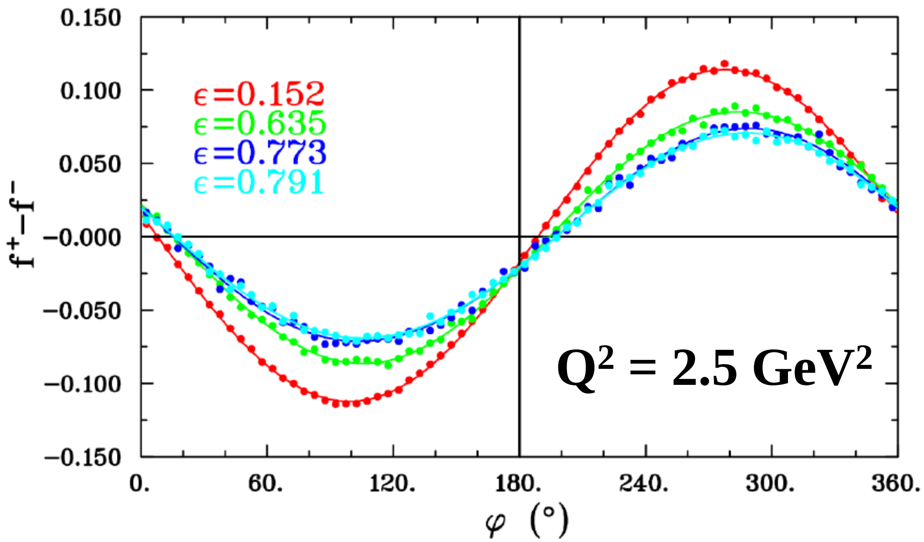

$$f_+ - f_- = \frac{N_{bins}}{2}\left[\frac{N_+(\varphi)}{N_0^+} - \frac{N_-(\varphi)}{N_0^-}\right]$$
$$= P_e \bar{A}_y \left(P_y^{FPP}\cos\varphi - P_x^{FPP}\sin\varphi\right)$$

Beam helicity reversal cancels false asymmetry

Analysis—FPP Analyzing Power

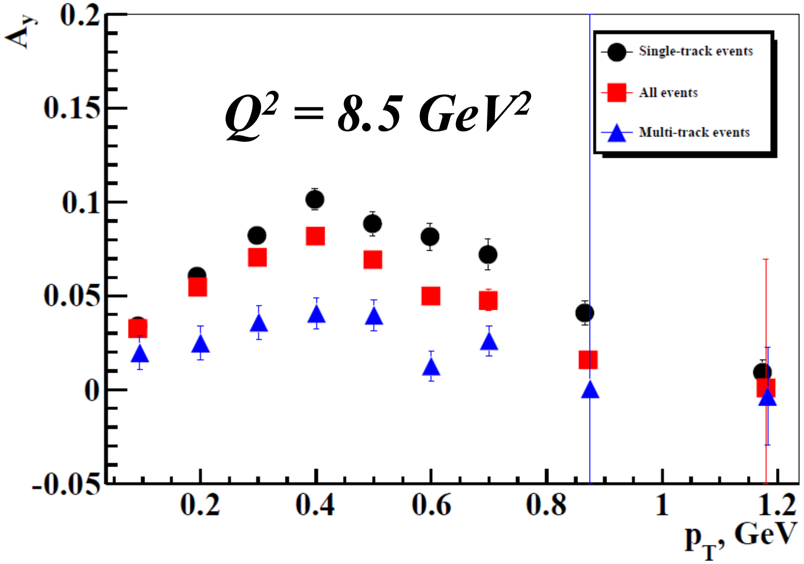

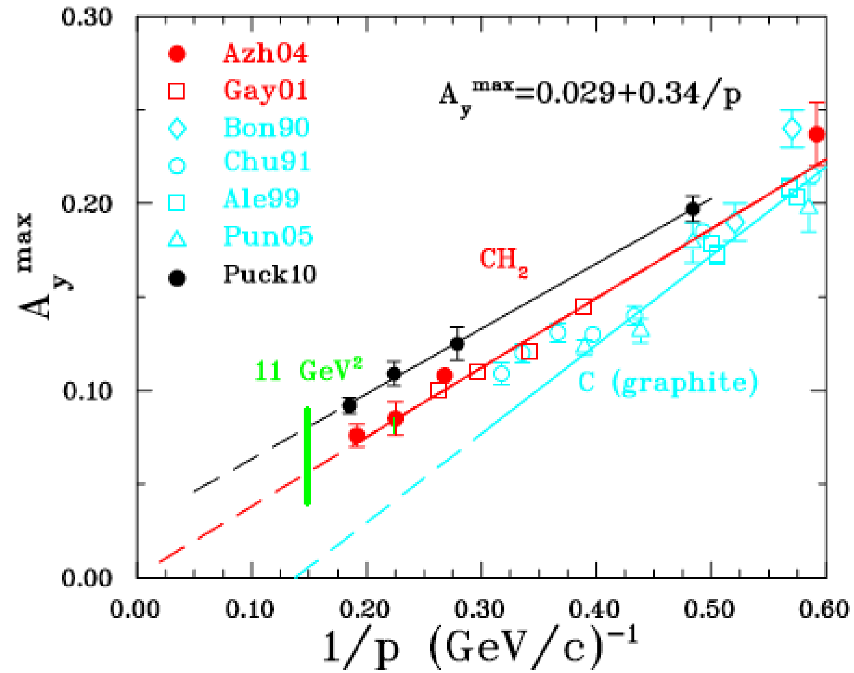

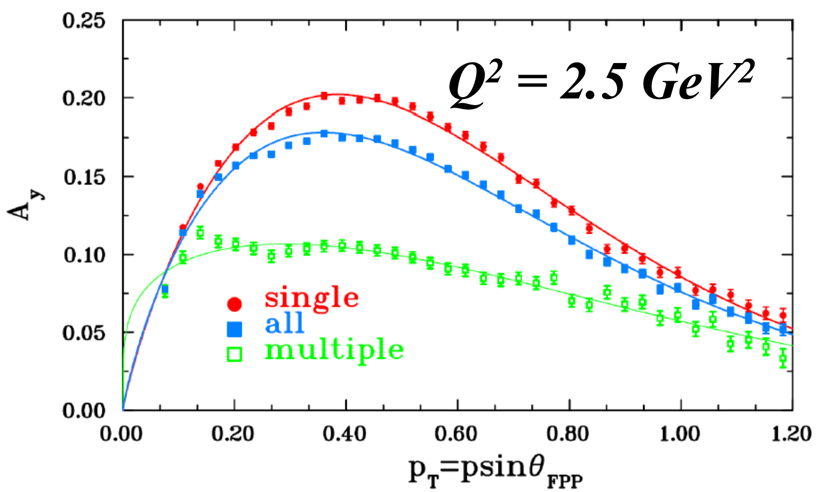

- Analyzing power of Hall C FPP increased relative to previous expts—ability to differentiate single/multi-track events

Analysis—Spin Precession I

$$\frac{d\mathbf{S}}{dt} = \frac{e}{m\gamma}\mathbf{S} \times \left[\frac{g}{2}\mathbf{B}_{\parallel} + \left(1 + \gamma\left(\frac{g}{2} - 1\right)\right)\mathbf{B}_{\perp}\right]$$

BMT Equation

$$\frac{d\mathbf{S}}{dt} = \gamma\left(\frac{g}{2} - 1\right)\left[\frac{e}{m\gamma}\mathbf{S} \times \mathbf{B}_{\perp}\right]$$

BMT equation in comoving coordinates, assuming $B_{\parallel} = 0$

Q^2, GeV^2	p_0, GeV/c	χ_θ, °
2.5	2.0676	108.5
5.2	3.5887	177.2
6.7	4.4644	217.9
8.5	5.4070	262.2

Central precession angles in GEp-III/2γ Experiments

- FPP asymmetry measures proton polarization *after* undergoing precession in HMS magnets
  - Precession makes P_L measurement possible by rotating longitudinal into transverse
- Calculation of spin transport through HMS is the largest source of systematic uncertainty in all PT experiments to date.

Analysis—Spin Precession II

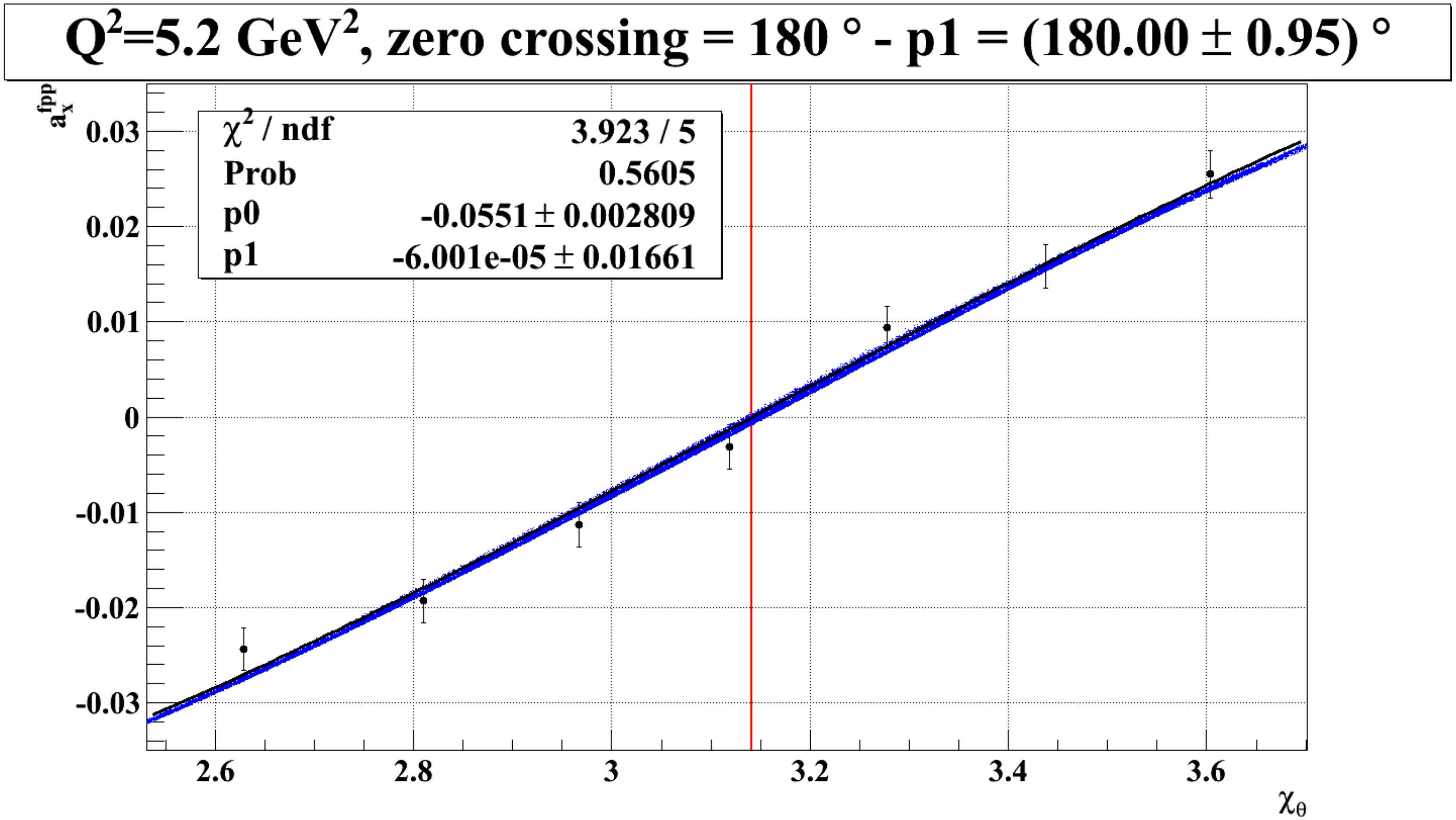

- $Q^2 = 5.2\ \text{GeV}^2$ kinematics chosen for overlap with Hall A *and* for central χ near 180˚--important consistency check of spin transport calculation

Analysis—Spin Precession, III

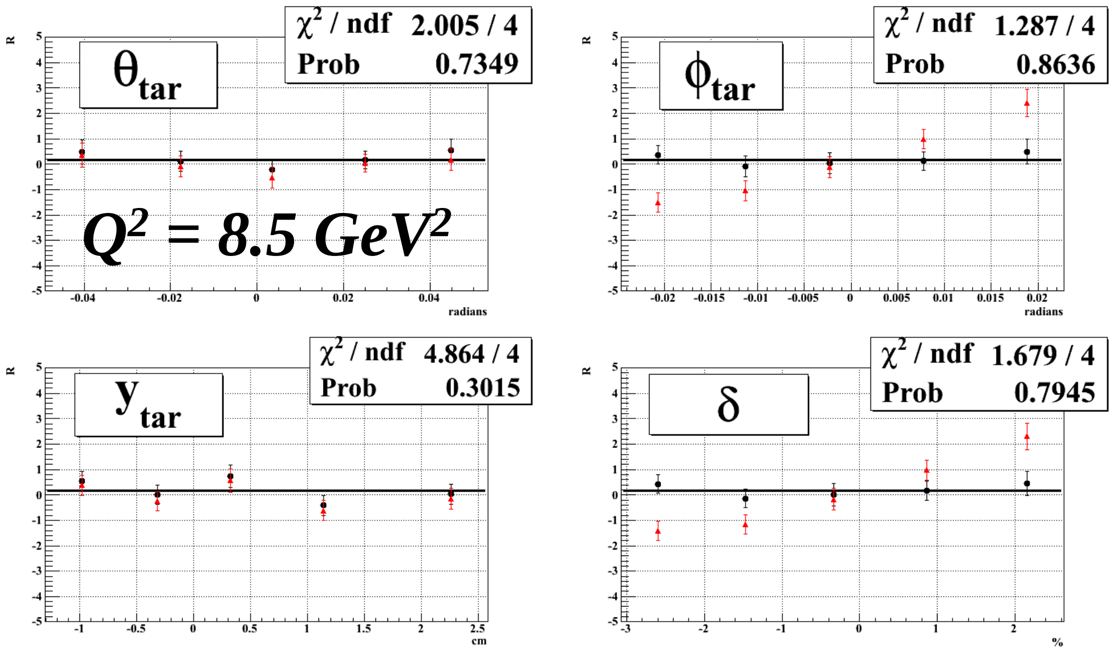

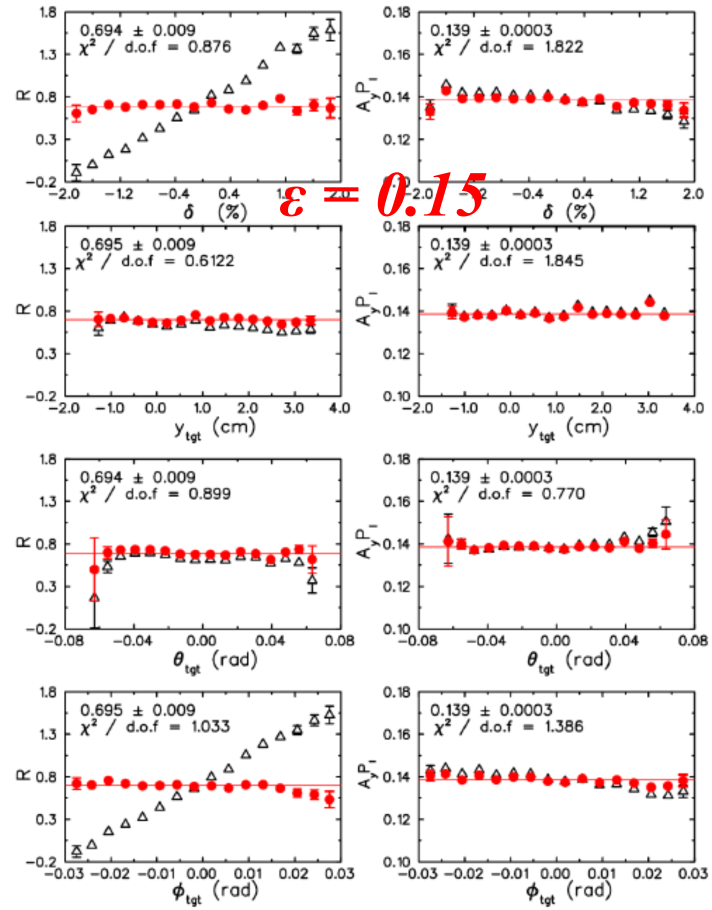

$Q^2 = 2.5$ GeV^2

- Extracted ratio P_T/P_L is very sensitive to quadrupole effects
- ***Absence of anomalous dependence of R on reconstructed proton kinematics is a powerful data quality check for spin transport calculation***

Analysis—Spin Precession, III

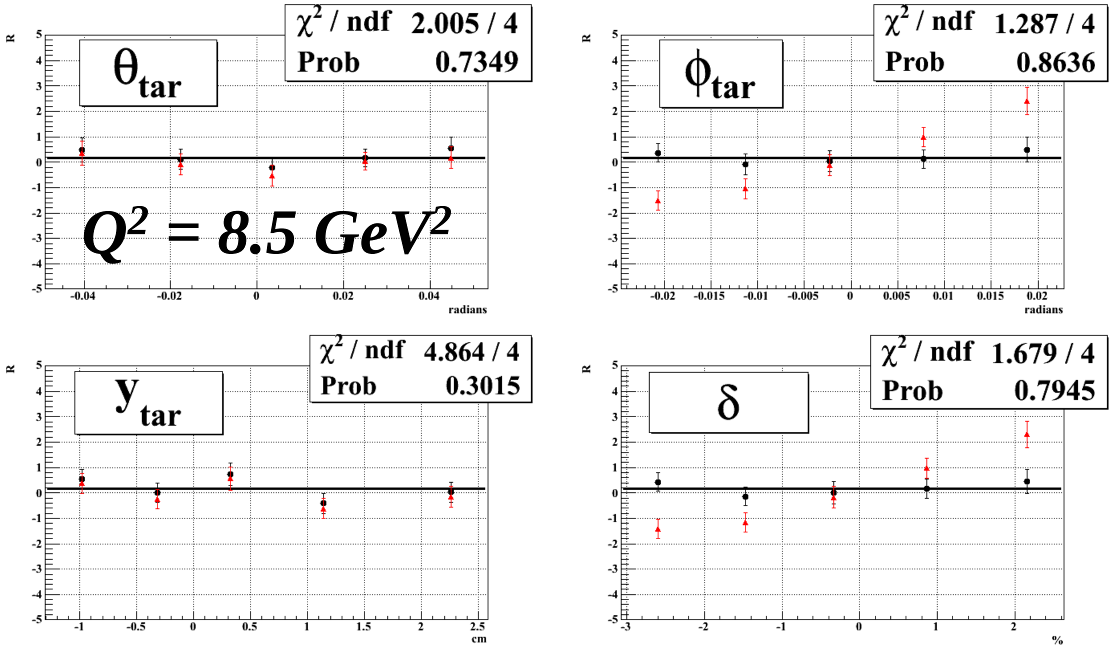

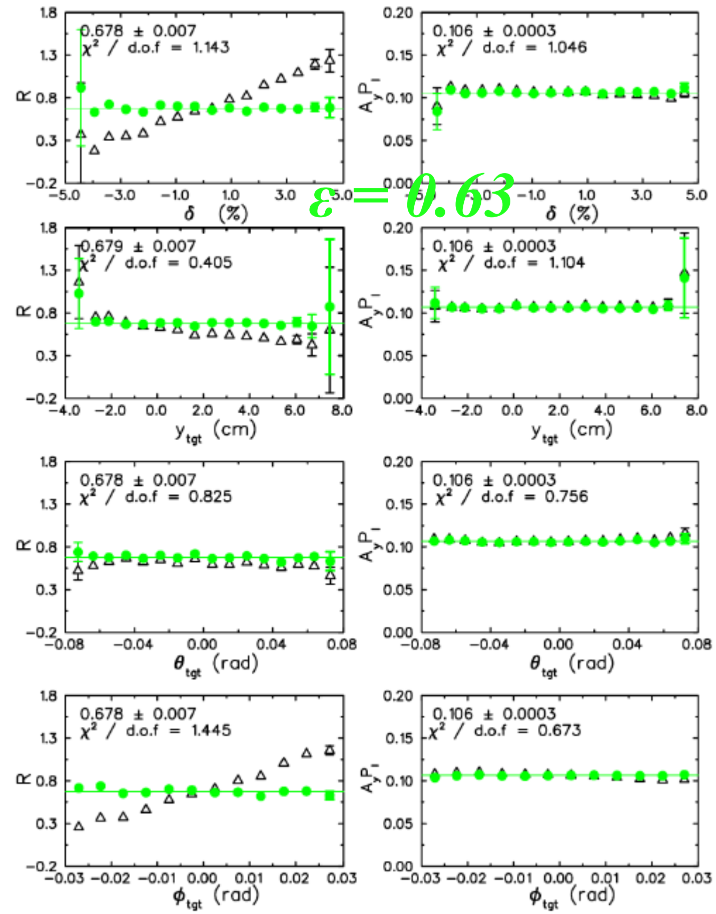

- Extracted ratio P_T/P_L is very sensitive to quadrupole effects
- ***Absence of anomalous dependence of R on reconstructed proton kinematics is a powerful data quality check for spin transport calculation***

$Q^2 = 2.5$ GeV^2

Analysis—Spin Precession, III

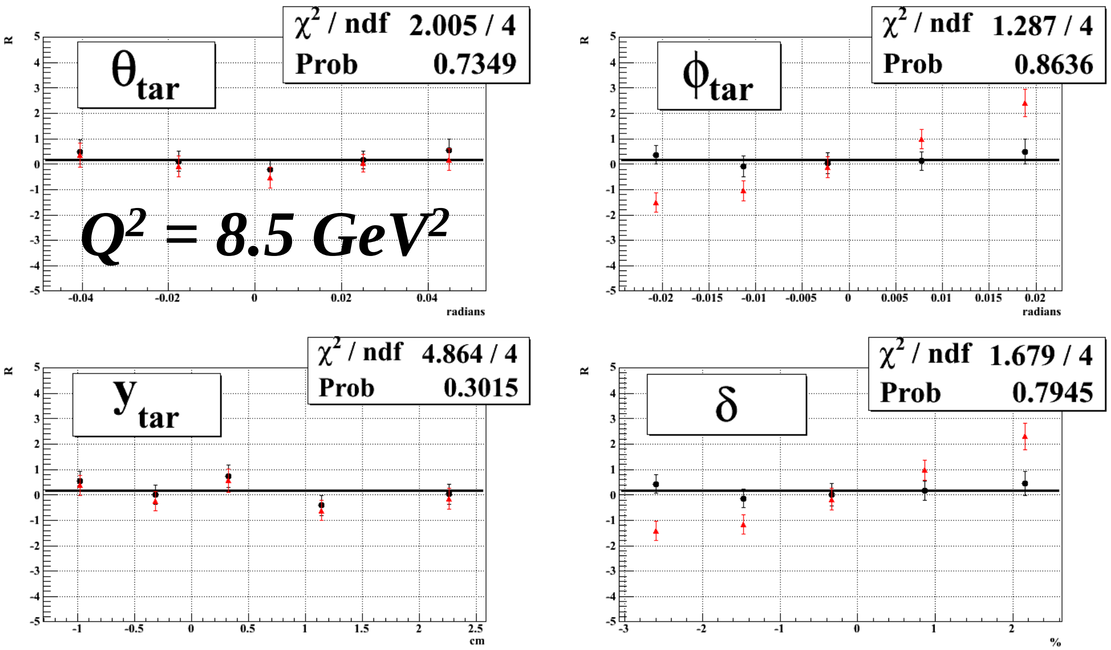

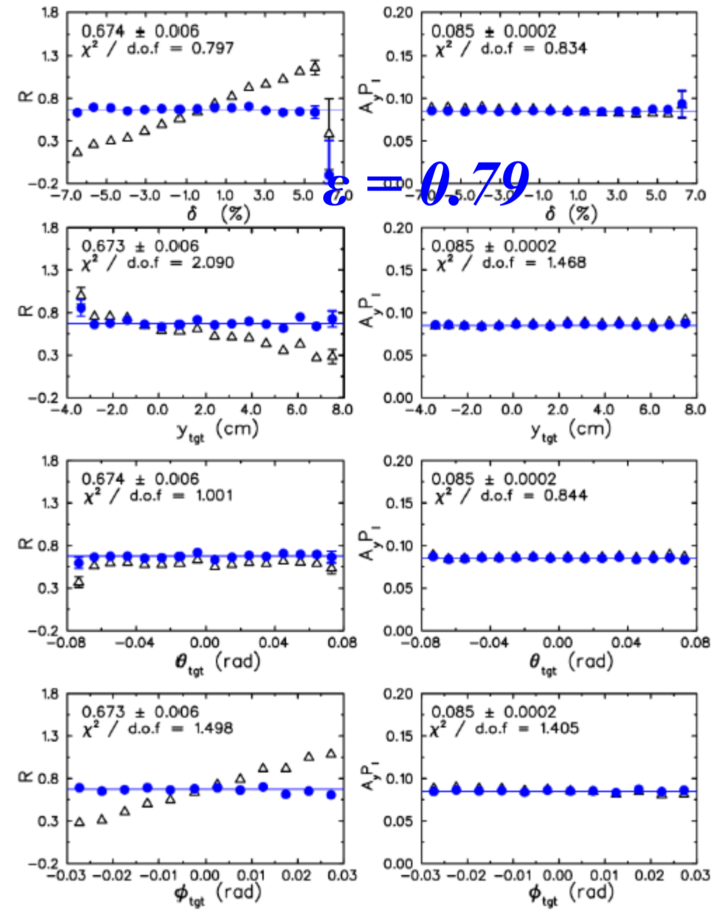

- Extracted ratio P_T/P_L is very sensitive to quadrupole effects
- ***Absence of anomalous dependence of R on reconstructed proton kinematics is a powerful data quality check for spin transport calculation***

$Q^2 = 2.5$ GeV^2

GEp-III Results: PRL 104, 242301 (2010)

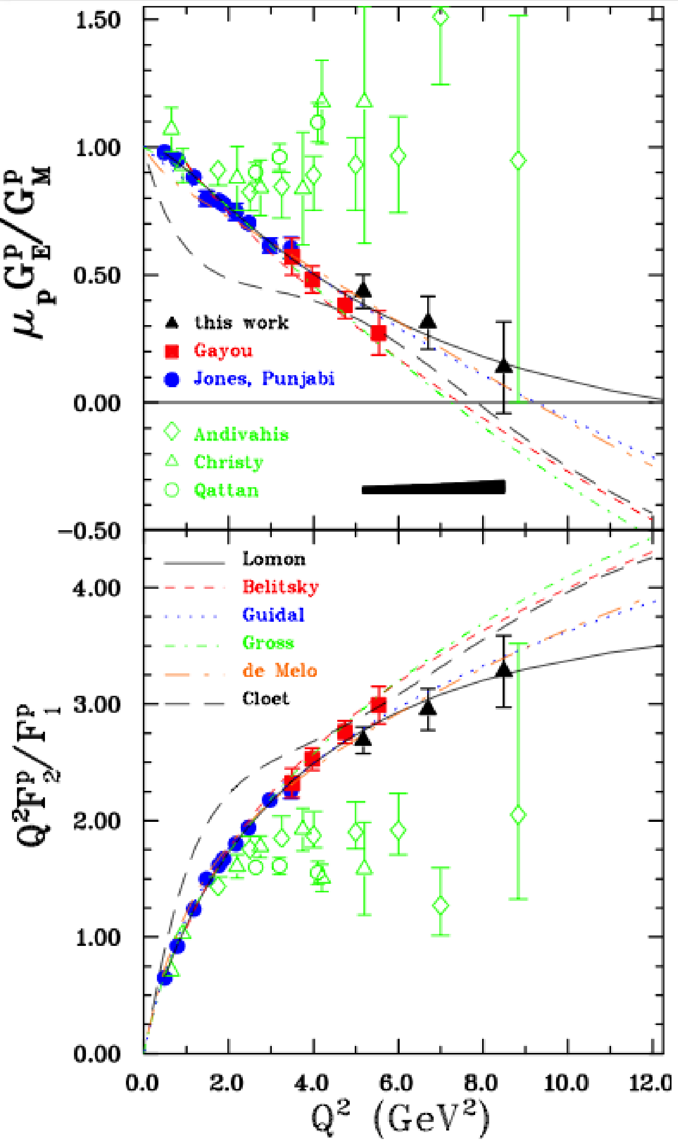

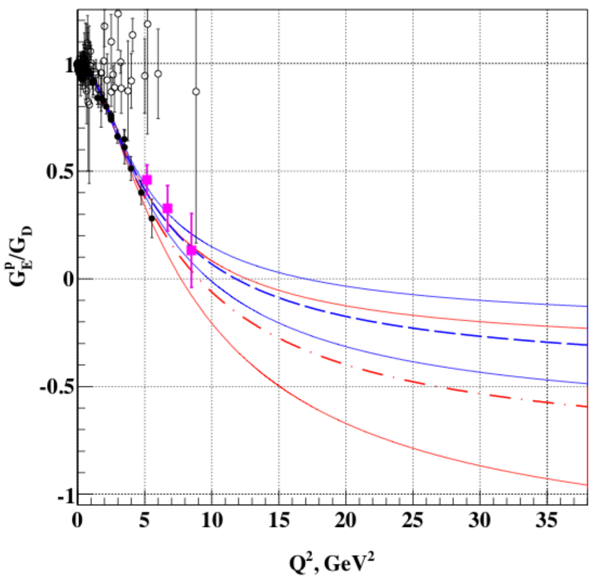

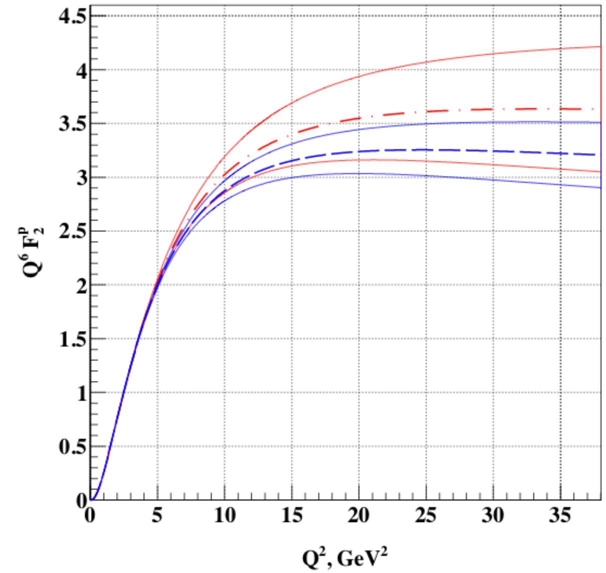

- Increased Q^2 coverage of the data by ~50%
- All three points at least 1.5σ above Gayou linear fit to GEp-I/II data
- Rate of decrease of G_{Ep}/G_{Mp} slowing down
- Error bars in high-Q^2/asymptotic G_{Ep}/F_{2p} reduced by ~factor of 2 in a global analysis using the Kelly fit.
- As the first high-Q^2 data outside Hall A, did these results point to a consistency issue between Halls A and C?

Reanalysis of GEp-II Data

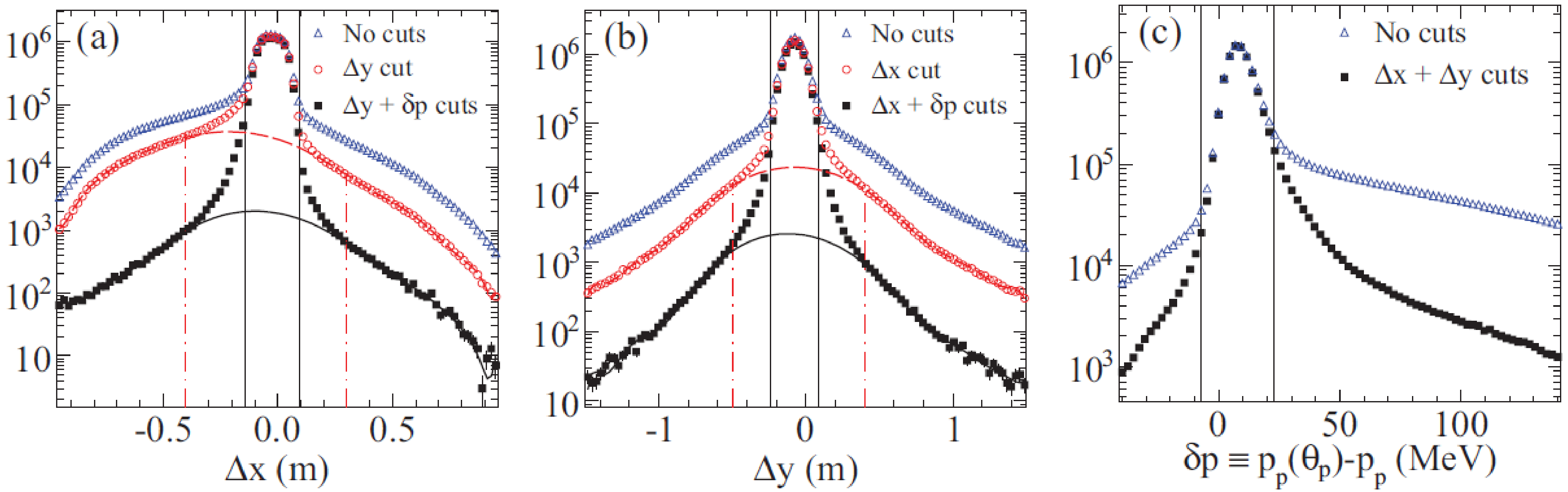

- Elastic event selection in GEp-II: similar to GEp-III but with different dominant sources of resolution
- $\gamma p \rightarrow \pi^0 p$ background led to important corrections in GEp-III; proton $p(\theta) - p$ cut found crucial, but *no such cut* was applied in original GEp-II analysis

Effect of the underestimated background

- Most events outside the elastic peak of $\delta p = p(\theta) - p$ are background-dominated.
- The observed polarization components evolve from those of the signal to those of the background as δp increases
- Net systematic effect is ~15% in P_T, 2% in P_L
- Conclusions borne out by Monte Carlo:

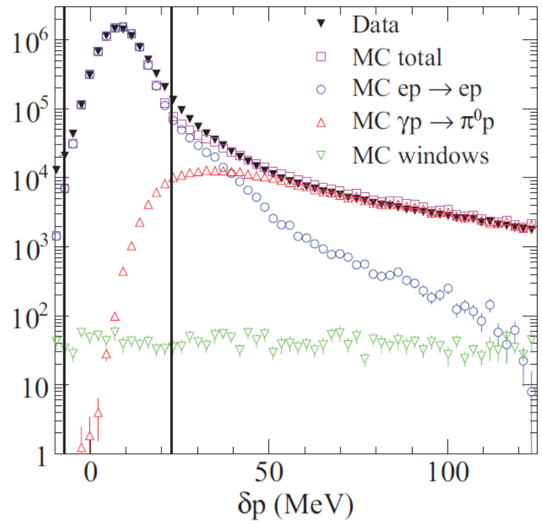

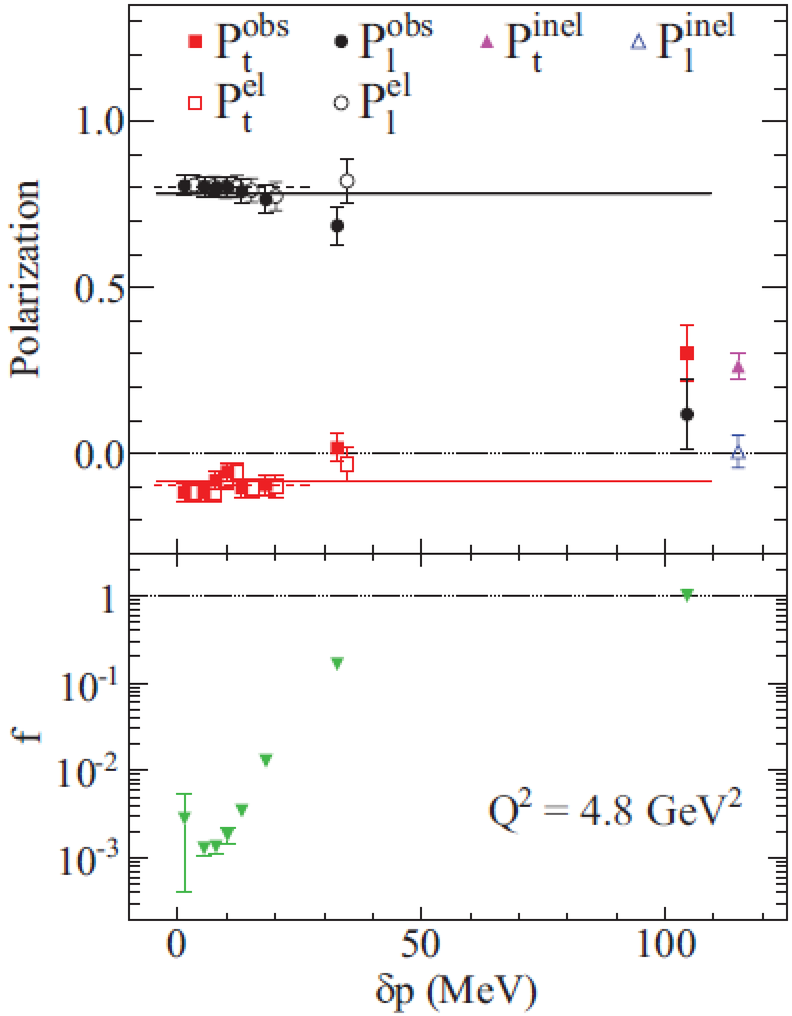

Final Results of GEp-II

Summary of results

- Reanalyzed three highest-Q^2 points (electron detected in calorimeter)
- Lowest $Q^2 = 3.5$ GeV^2 not reanalyzed (electron detected in HRSR).
- Three highest-Q^2 R values systematically increase, by several times the originally quoted systematics.
- ***Increase mainly due to previously underestimated background***
- Addition of $p(\theta) - p$ cut suppresses background to <0.4%, remaining correction and uncertainty small
- Consistency of GEp-I/II/III/2γ data (Hall A vs. Hall C) is now excellent in a wide Q^2 range
- ***Updated analysis and results now published in Phys. Rev. C, PRC 85, 085, 045203***

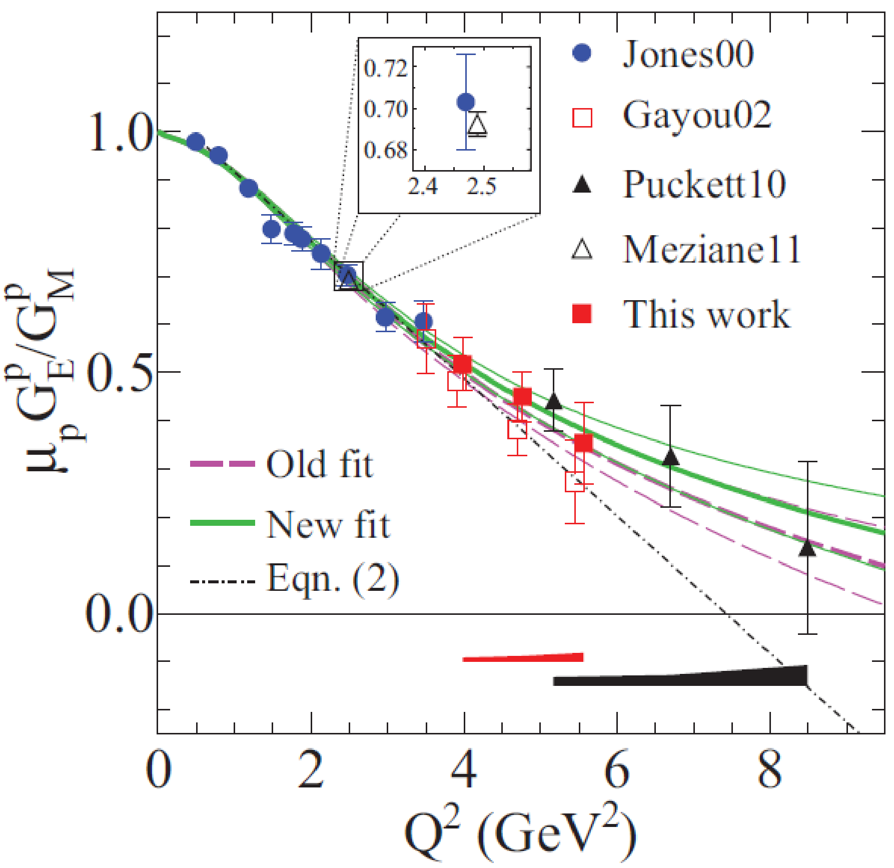

Current Status of Nucleon FF Data/Theory

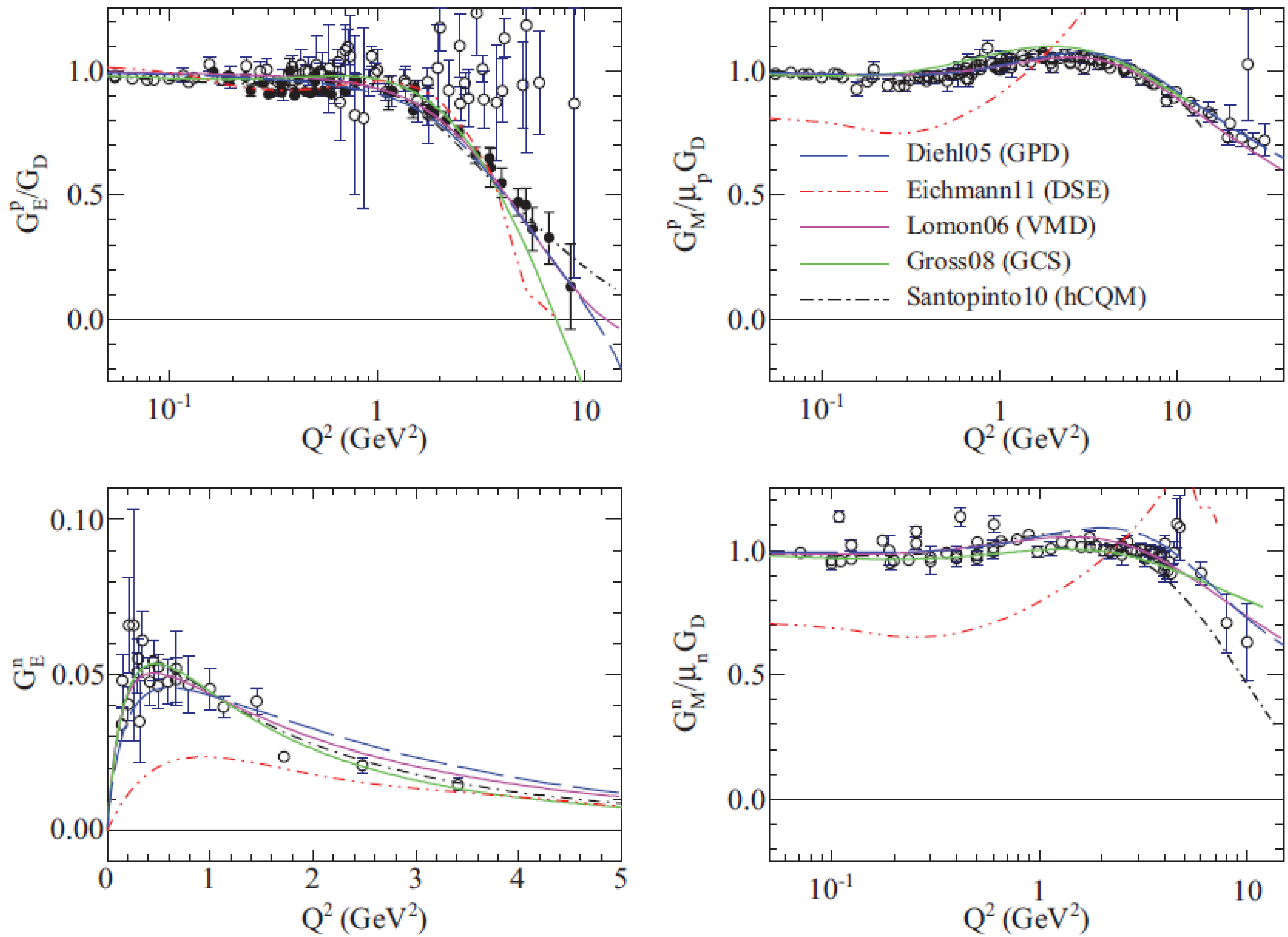

How to go to higher Q^2?

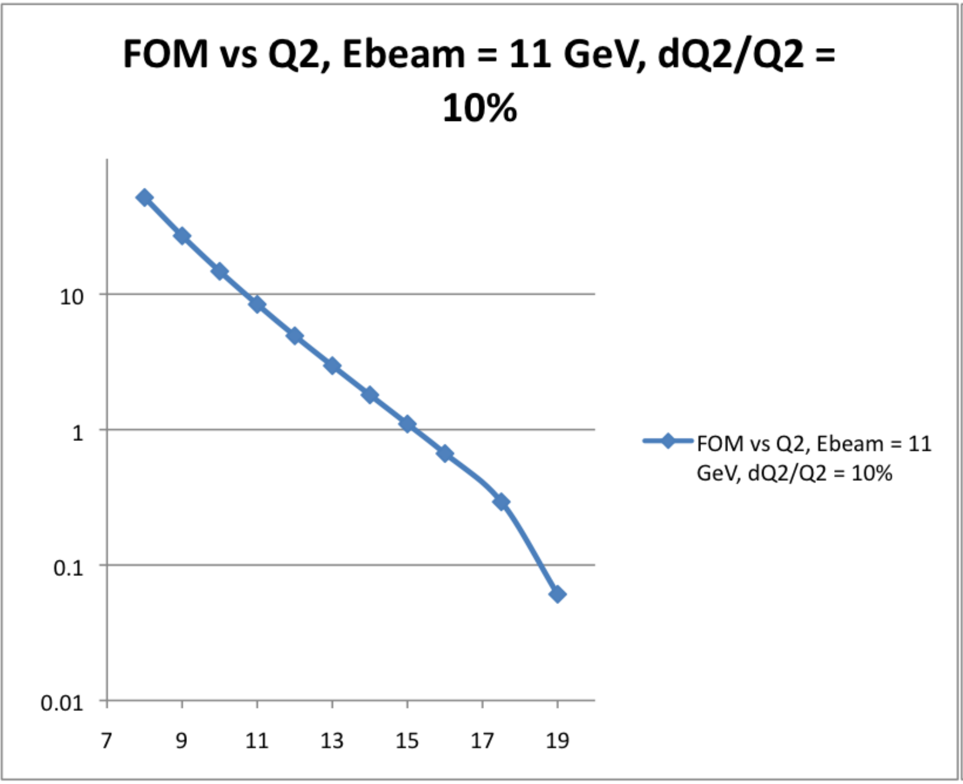

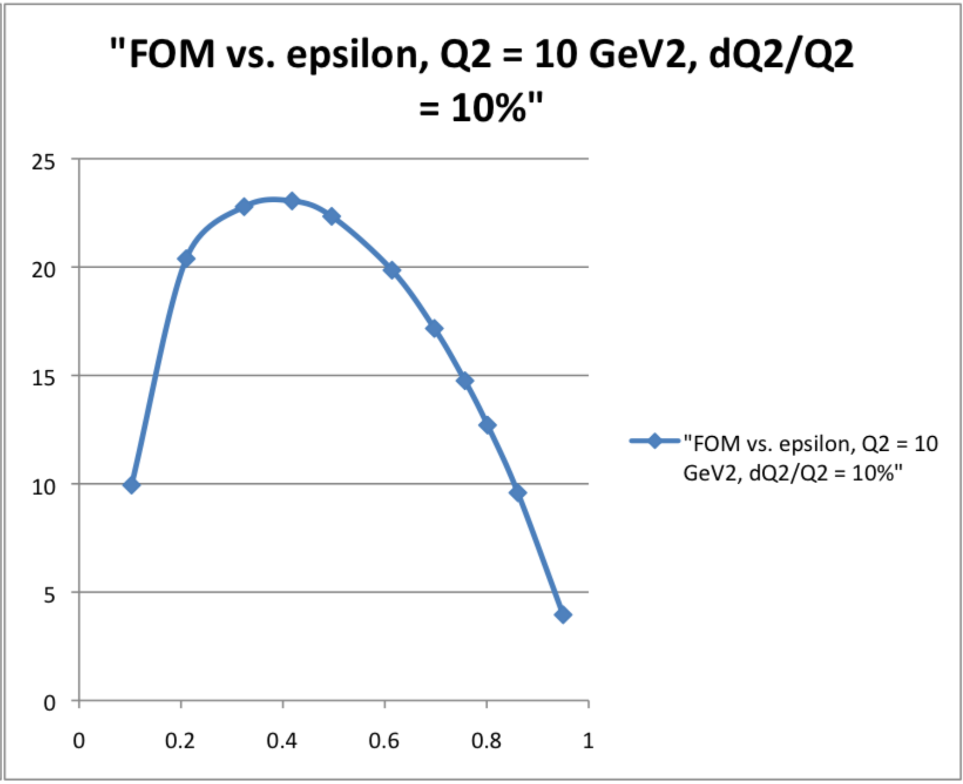

FOM vs. Q^2 at E = 11 GeV (a. u.) FOM vs. ε at Q^2 = 10 GeV^2 (a. u.)

- Must increase luminosity and acceptance to compensate for E^2/Q^{16} dependence of (cross section * A_y^2 contributions to) figure of merit

GEp-V: The Final Frontier

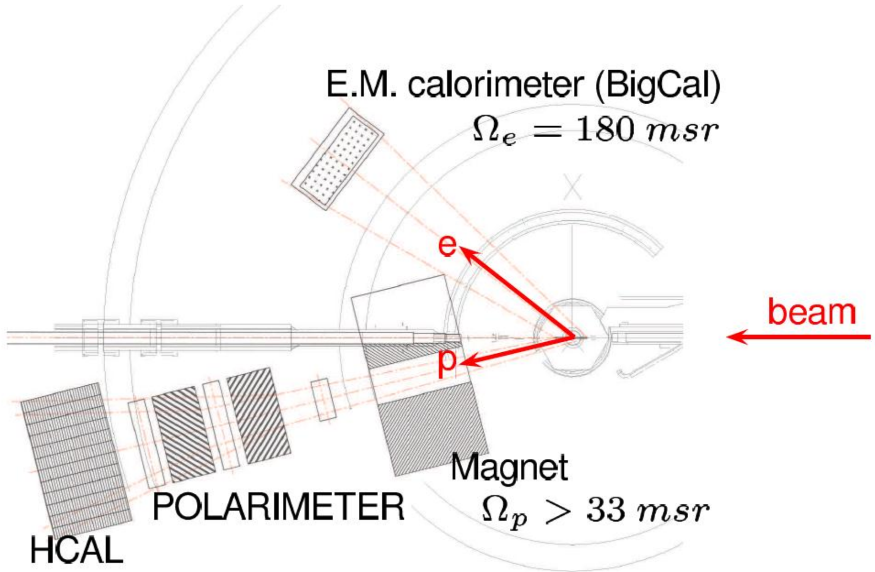

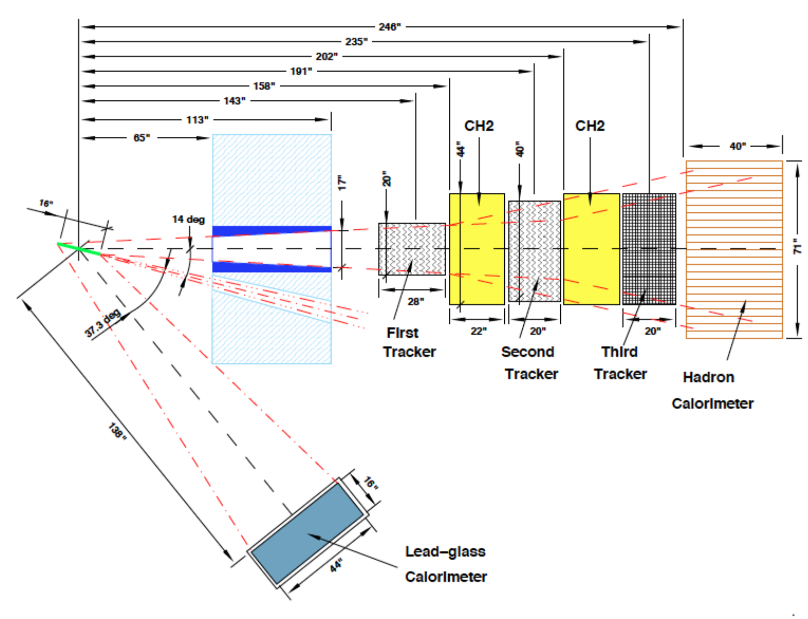

Figure 5.1: The location and dimension of the GEp(5) experiment components.

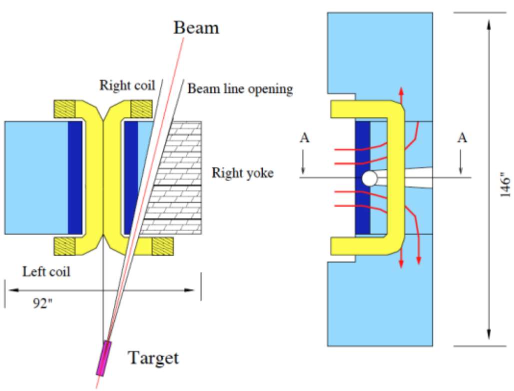

Figure 3.2: The concept of the beam path through the dipole.

- At large Q^2, the proton in ep elastic scattering goes to forward angles at high momentum.
- New "Super BigBite" spectrometer: Open-geometry, vertical-bend dipole spectrometer
- High-rate tracking based on GEM technology.
- New FPP with full geometric acceptance for angles up to 10°
- ***Spokespersons: B. Wojtsekhowski (contact), L. Pentchev, C. F. Perdrisat, V. Punjabi, M. K. Jones, E. Cisbani, E. Brash, ...***

Projected Results Approved by JLab PAC

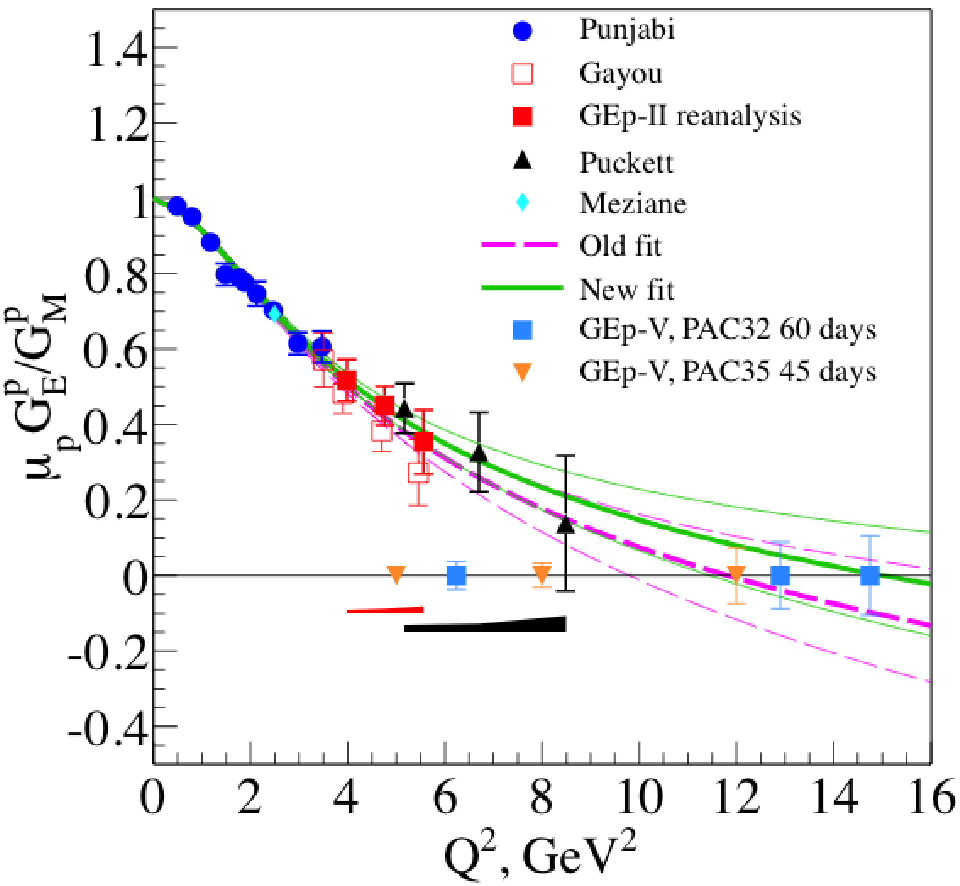

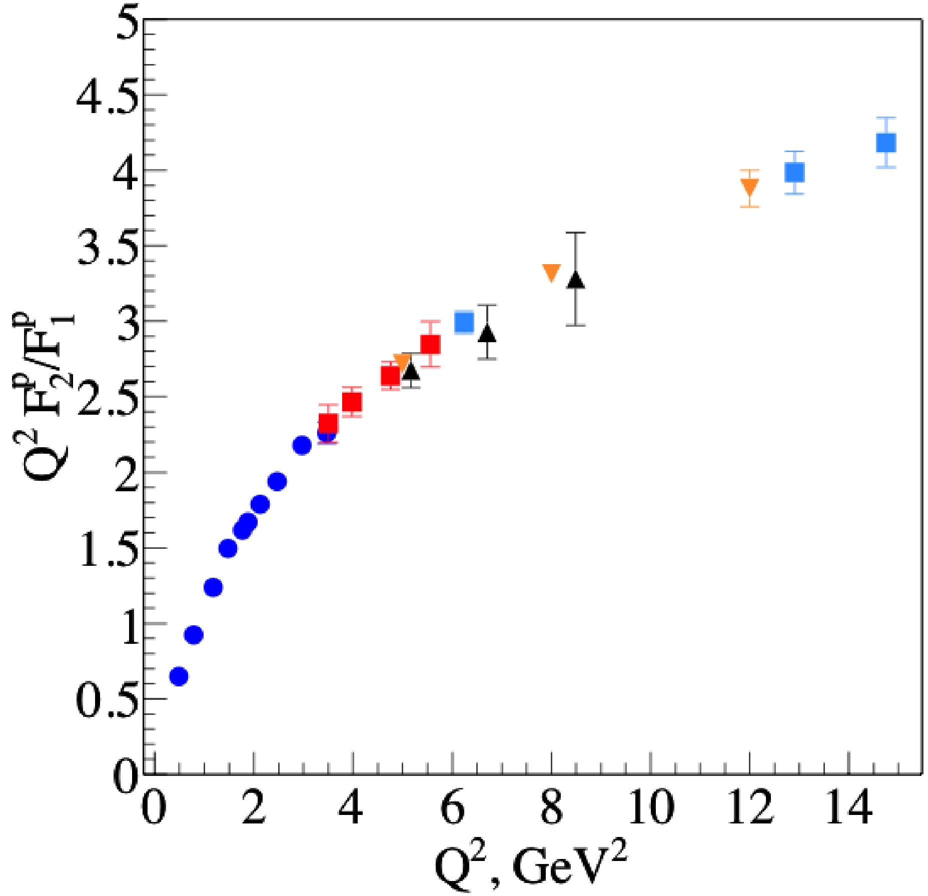

Projected results as $\mu G_E/G_M$

Projected results as $Q^2\ F_2/F_1$

OPPORTUNITIES WITH CLAS12 @ JLAB HALL B

ep→ep in CLAS12 @ 11 GeV

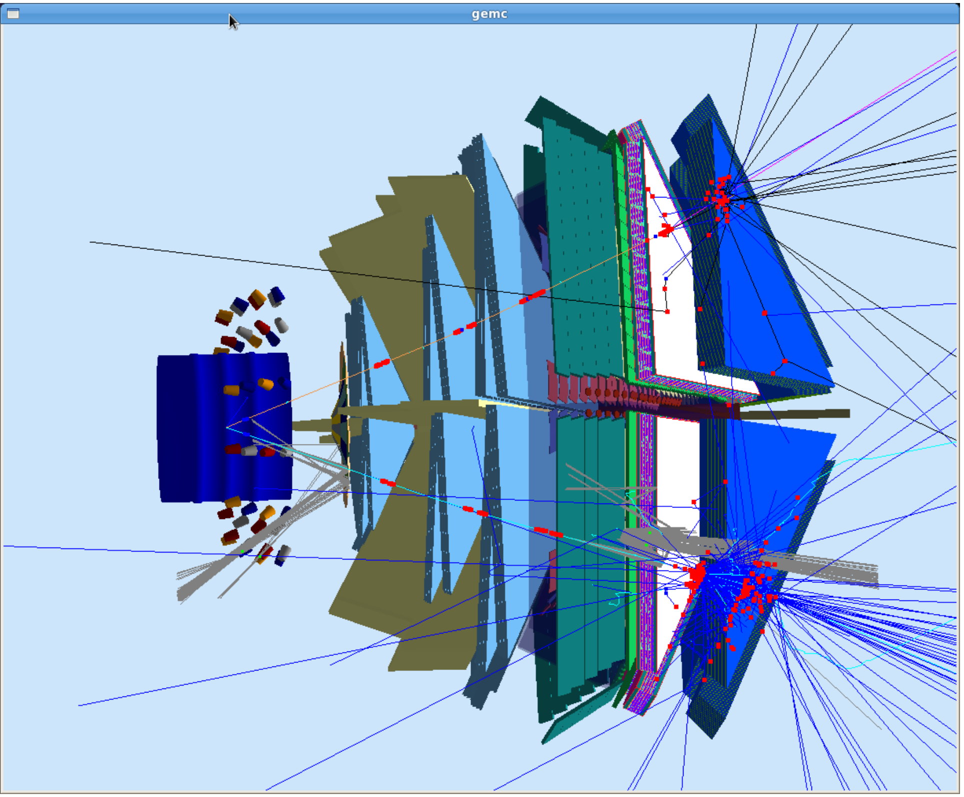

Elastic ep→ep in gemc

- Standard detector/magnetic field configuration (inbending e^-)
- ELRADGEN2.0 rad. corr. (internal only)

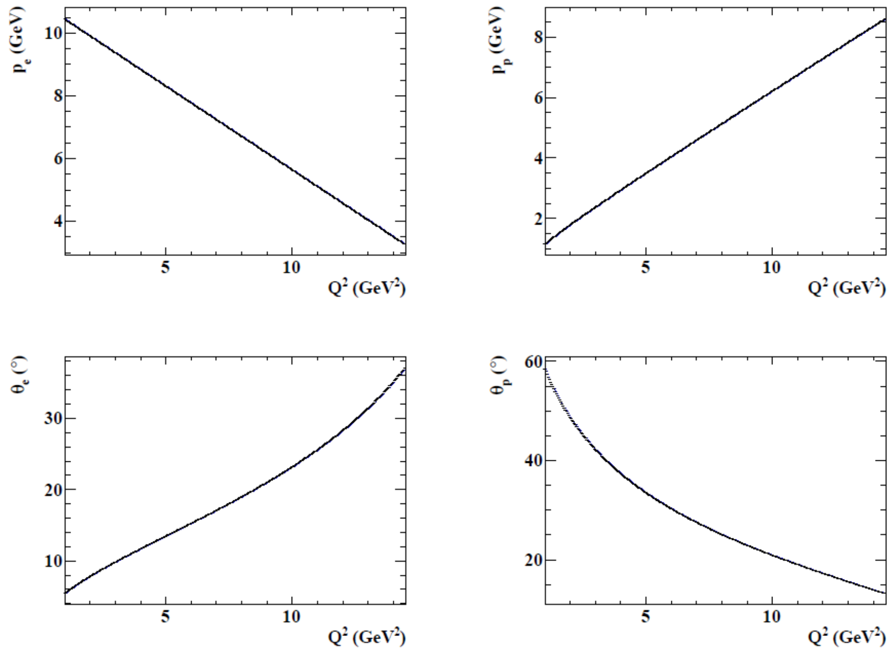

- Scattered electron and proton kinematics vs. Q^2 at E_{beam} = 11 GeV
- Forward CLAS12 acceptance ~2-14 GeV^2 (electrons)

Normal Single-Spin Asymmetry in ep→ep

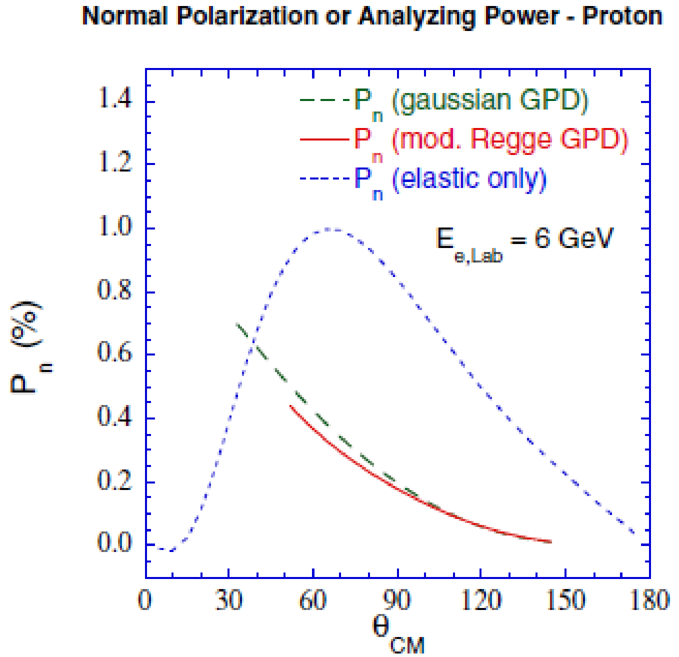

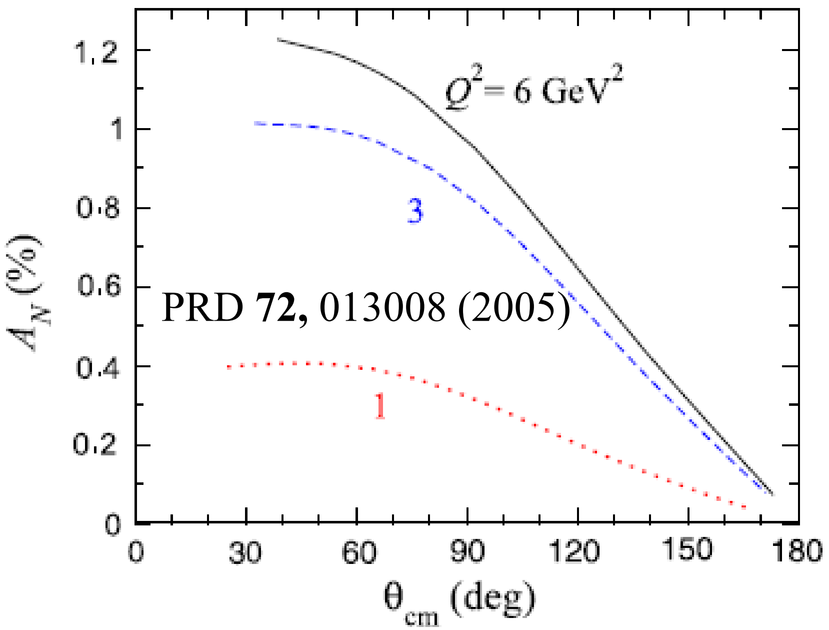

Elastic and GPD A_N vs θ, fixed E

Elastic A_N vs θ, fixed Q^2

- A_N = single-spin asymmetry in elastic scattering when proton polarization is normal to the scattering plane
- ***Identically zero in one-photon-exchange approximation—clean signal for Im(TPEX)***
- Equal to induced normal recoil polarization in unpolarized ep→ep (time reversal)
- No data currently exist (due to challenges of tranversely polarized targets).
- Induced recoil polarization very difficult to measure due to polarimeter false asymmetries

CLAS12 acceptance for ep→ep @ 11 GeV

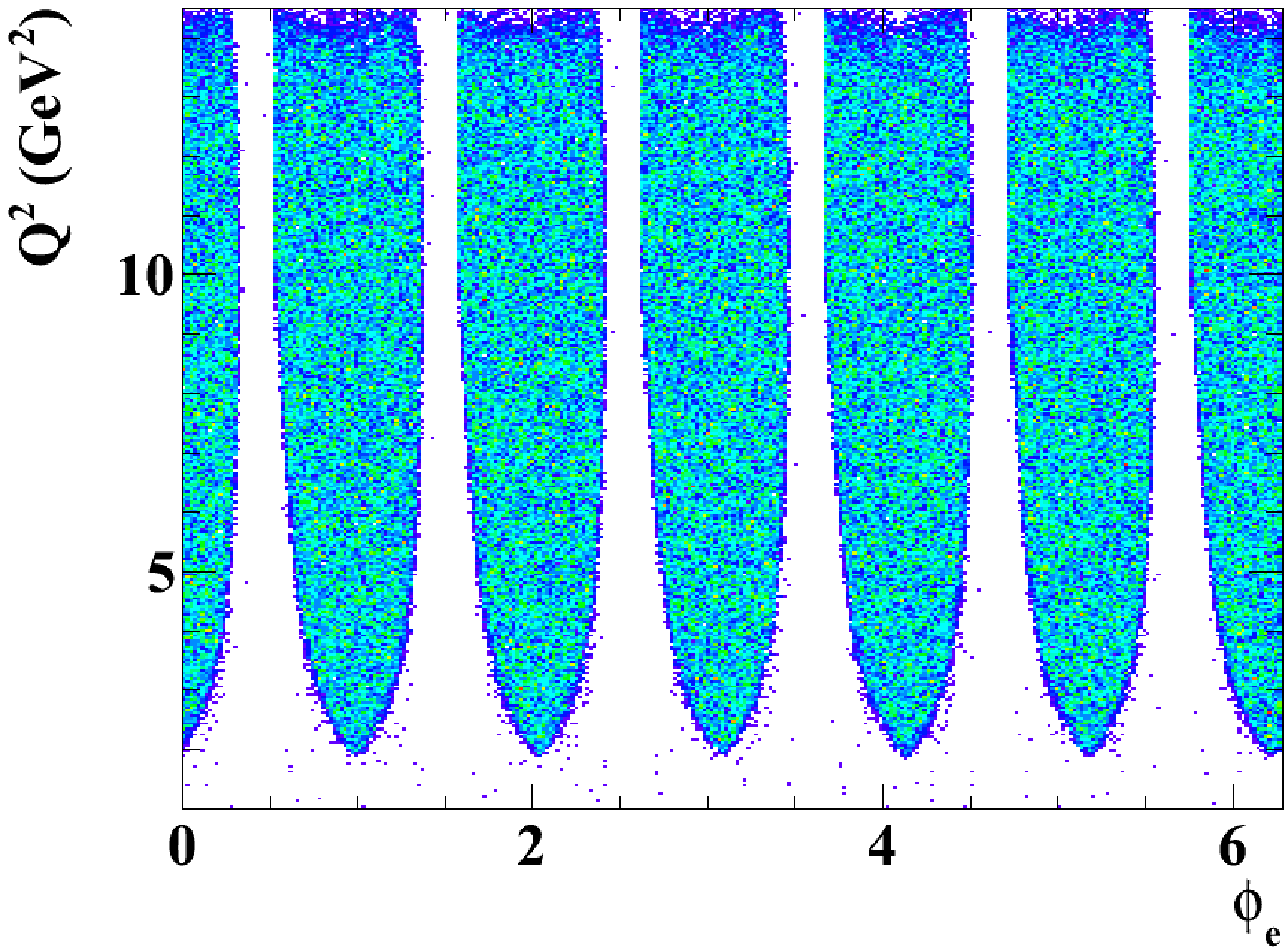

Transversely Polarized HD-Ice Target

HD-Ice target vs standard nuclear targets (less luminosity for higher purity)

Advantages:

- Minimize nuclear background
  smaller dilution, no attenuation at large p_T
- Weak holding field (BdL ~ 0.1 Tm)
  wide acceptance, negligible beam deflection

Deuterium dilution is under control
E12-06-112

Suitable for di-hadron and recoil proton
PR12-12-009/010

Disadvantages:

- Very long polarizing times (months)
- Sensitivity to local heating by charged beams

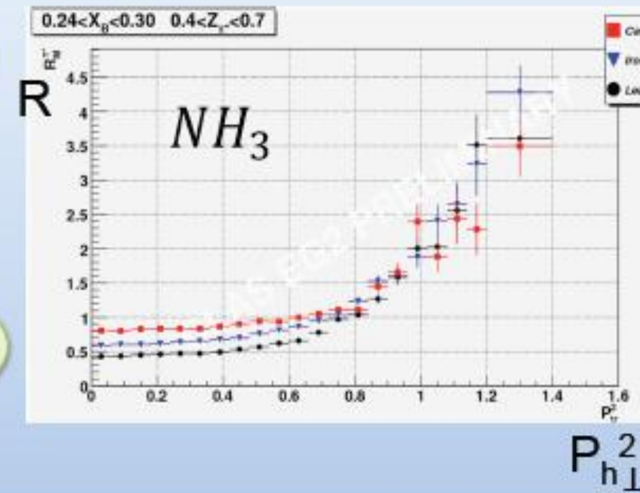

HD-ice ran from Nov/11 to May/12 at Jlab with 15mm Ø ×50 mm long HD cells

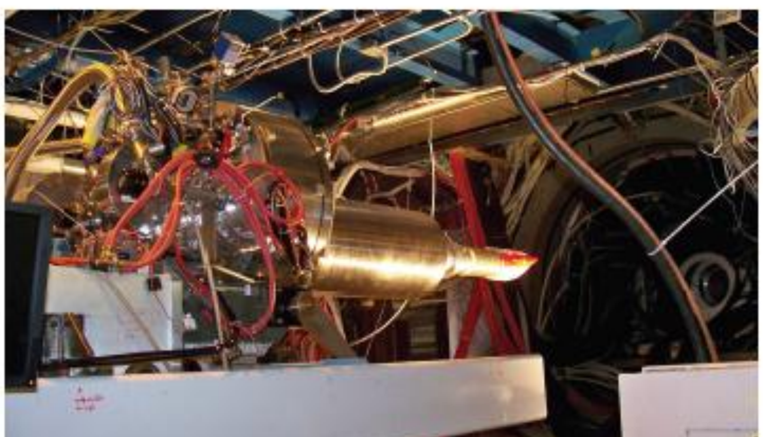

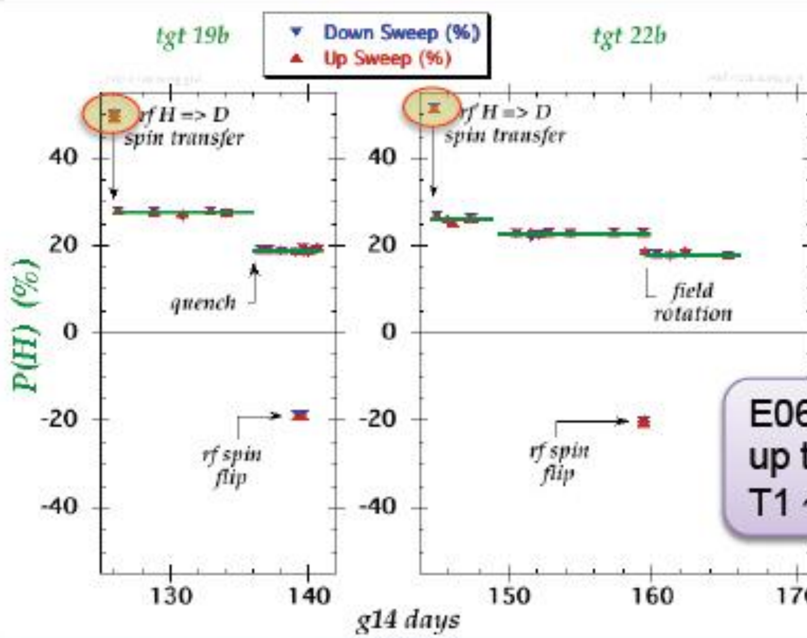

E06-101
up to 10^8 γ/s
T1 ~ years

Asymmetry Projections

- Assumptions:
  – 100 days @ 10^{34} Hz/cm^2 (for various reasons this may be overly optimistic)
  – Target Polarization = 60% up vertical
  – Beam Polarization = 85% longitudinal
- Measured asymmetries depend on both Q^2 and azimuthal scattering angle:
  – A_N is modulated by the cosine of the angle between the scattering plane and the target spin
  – Beam-target double-spin asymmetry A_{beam} depends on orientation of target spin relative to **q**

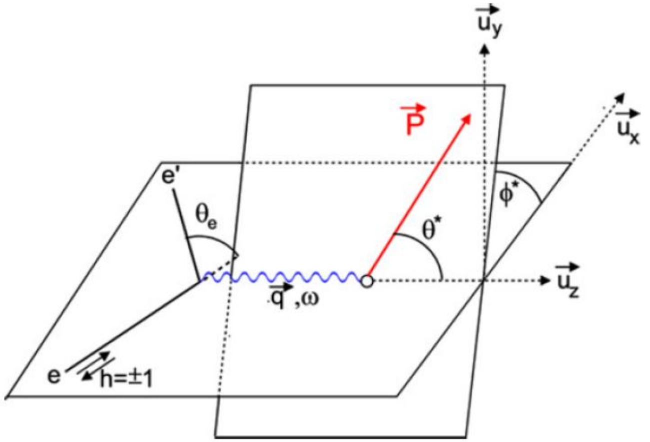

$$A_N \propto P_p \sin\theta^* \sin\phi^*$$

$$A_{beam} = -\frac{P_e P_p}{1+\frac{\epsilon r^2}{\tau}}\left[\sqrt{\frac{2\epsilon(1-\epsilon)}{\tau}}\sin\theta^*\cos\phi^* r + \sqrt{1-\epsilon^2}\cos\theta^*\right]$$

$$r = \frac{G_E^p}{G_M^p}$$

Advantage of transverse target: sensitivity to r increases with Q^2

A_N Q^2 Dependence

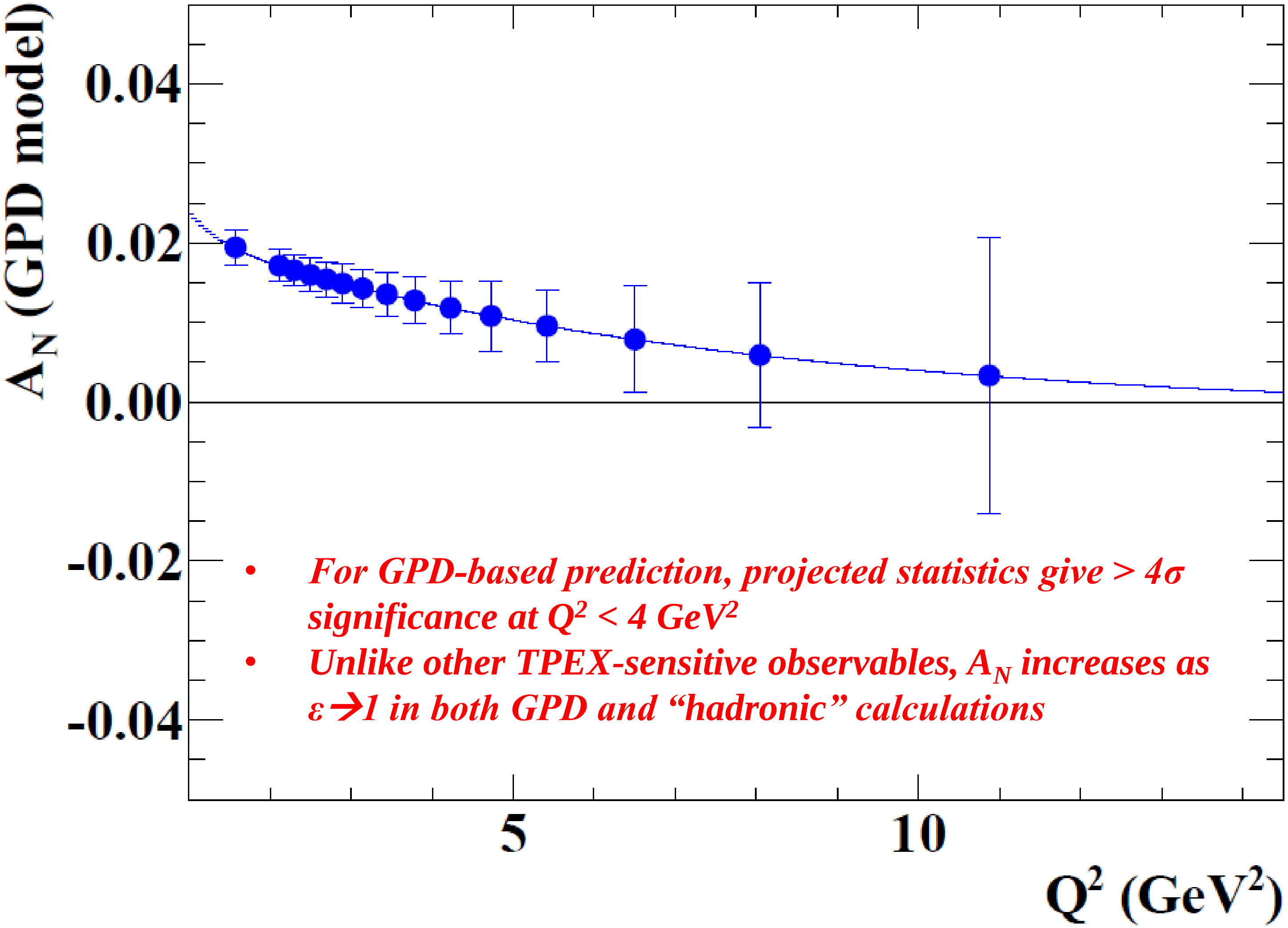

- *For GPD-based prediction, projected statistics give > 4σ significance at $Q^2 < 4$ GeV^2*
- *Unlike other TPEX-sensitive observables, A_N increases as $\varepsilon \rightarrow 1$ in both GPD and "hadronic" calculations*

G_{Ep}: Recoil vs. Polarized Target

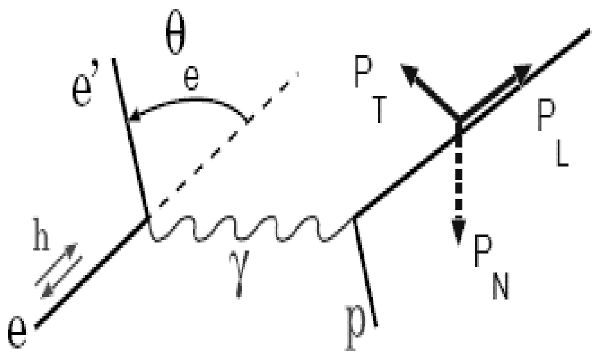

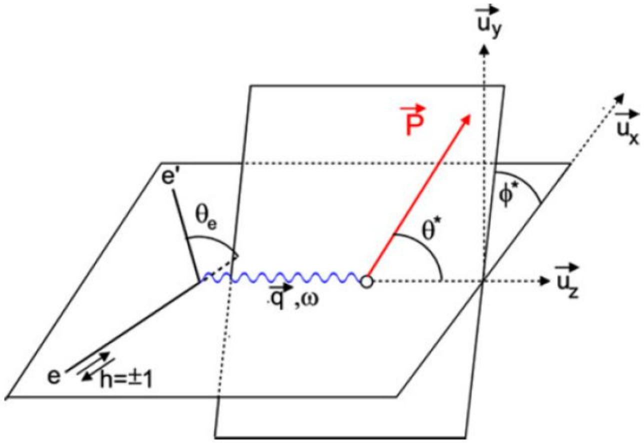

	Polarization Transfer	*Polarized Beam-Target Asymmetry*
Luminosity (Hz/cm^2)	$\sim 10^{39}$	$<\sim 10^{35}$ max.
Asymmetry Magnitude	$\sim P_{beam} A_y$ ($A_y \sim 1/Q^2$)	$\sim P_{beam} P_{target}$
Acceptance	Limited by proton arm: ~6 msr (HRS/HMS) or ~40 msr (SBS)	~4π (CLAS12)
Polarimeter efficiency	~25%	N/A
Systematics	Spin precession	Polarimetry/relative lumi.
Rad. Corr.	Very small	Small
TPEX Corr.	Small (GEp-2γ expt)	??

G_E/G_M: Projected Results

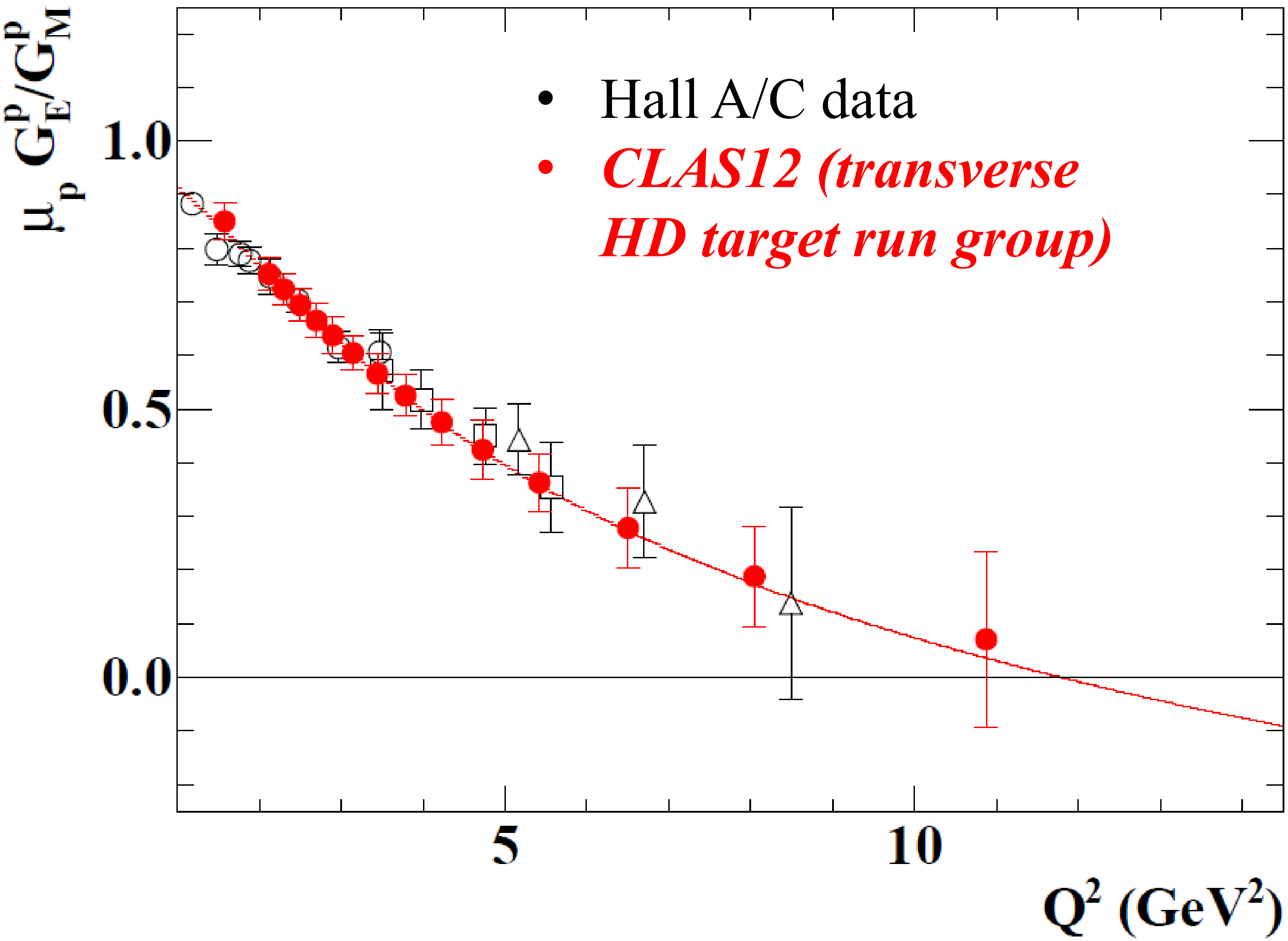

Summary/Conclusions

- The GEp-III experiment has significantly enhanced the knowledge of high-Q^2 G_{Ep}—and the motivation for a reanalysis of GEp-II which found improved consistency between Halls A/C
- The GEp-2γ experiment, in combination with precise Rosenbluth data, has placed unprecedented constraints on the TPEX amplitudes at $Q^2 = 2.5$ GeV^2.
- The Super BigBite Spectrometer (SBS) project, now funded by DOE/JLab, will provide the best, highest-Q^2 G_{Ep} data following the 12 GeV upgrade of JLab.
- Depending on performance in an electron beam, CLAS12+HDice has the potential to make world's first A_N measurement in ep→ep at high Q^2, and also measure G_{Ep}/G_{Mp} using a third method (polarized target) with competitive precision and Q^2 coverage.

Acknowledgements

- GEp-III/GEp-2γ Collaborations
- US DOE
- MIT Nuclear Interactions Group
- Jefferson Lab Hall B Group and the CLAS Collaboration
- Thanks to the organizers for this opportunity!

BACKUP SLIDES

A_N in GPD framework—handbag mechanism

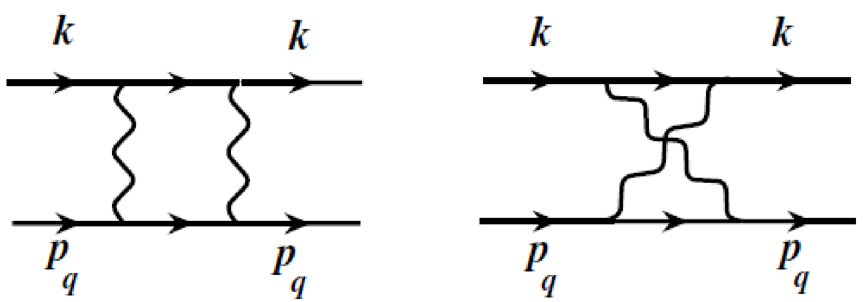

- The TPEX occurs at the parton level in eq → eq box diagram
- Parton process embedded in the nucleon via GPDs:

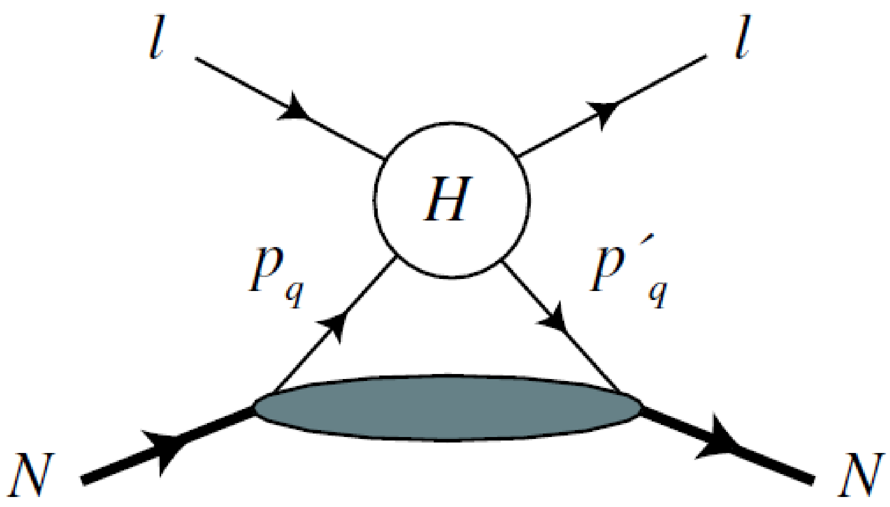

$$A_n = \sqrt{\frac{2\varepsilon(1+\varepsilon)}{\tau}}\frac{1}{\sigma_R}\left\{G_E I(A) - \sqrt{\frac{1+\varepsilon}{2\varepsilon}} G_M I(B)\right\},$$

$$A \equiv \int_{-1}^{1}\frac{dx}{x}\frac{[(\hat{s}-\hat{u})\tilde{f}_1^{\mathrm{hard}} - \hat{s}\,\hat{u}\,\tilde{f}_3]}{(s-u)}\sum_q e_q^2(H^q + E^q),$$

$$B \equiv \int_{-1}^{1}\frac{dx}{x}\frac{[(\hat{s}-\hat{u})\tilde{f}_1^{\mathrm{hard}} - \hat{s}\,\hat{u}\,\tilde{f}_3]}{(s-u)}\sum_q e_q^2(H^q - \tau E^q),$$

$$I(\tilde{f}_1^{\mathrm{hard}}) = -\frac{e^2}{4\pi}\left\{\frac{Q^2}{2\hat{u}}\ln\left(\frac{\hat{s}}{Q^2}\right) + \frac{1}{2}\right\},$$

$$I(\tilde{f}_3) = -\frac{e^2}{4\pi}\frac{1}{\hat{u}}\left\{\frac{\hat{s}-\hat{u}}{\hat{u}}\ln\left(\frac{\hat{s}}{Q^2}\right) + 1\right\}.$$

PRD **72,** 013008 (2005)

Counts for 100 days@10^{34} Hz/cm^2

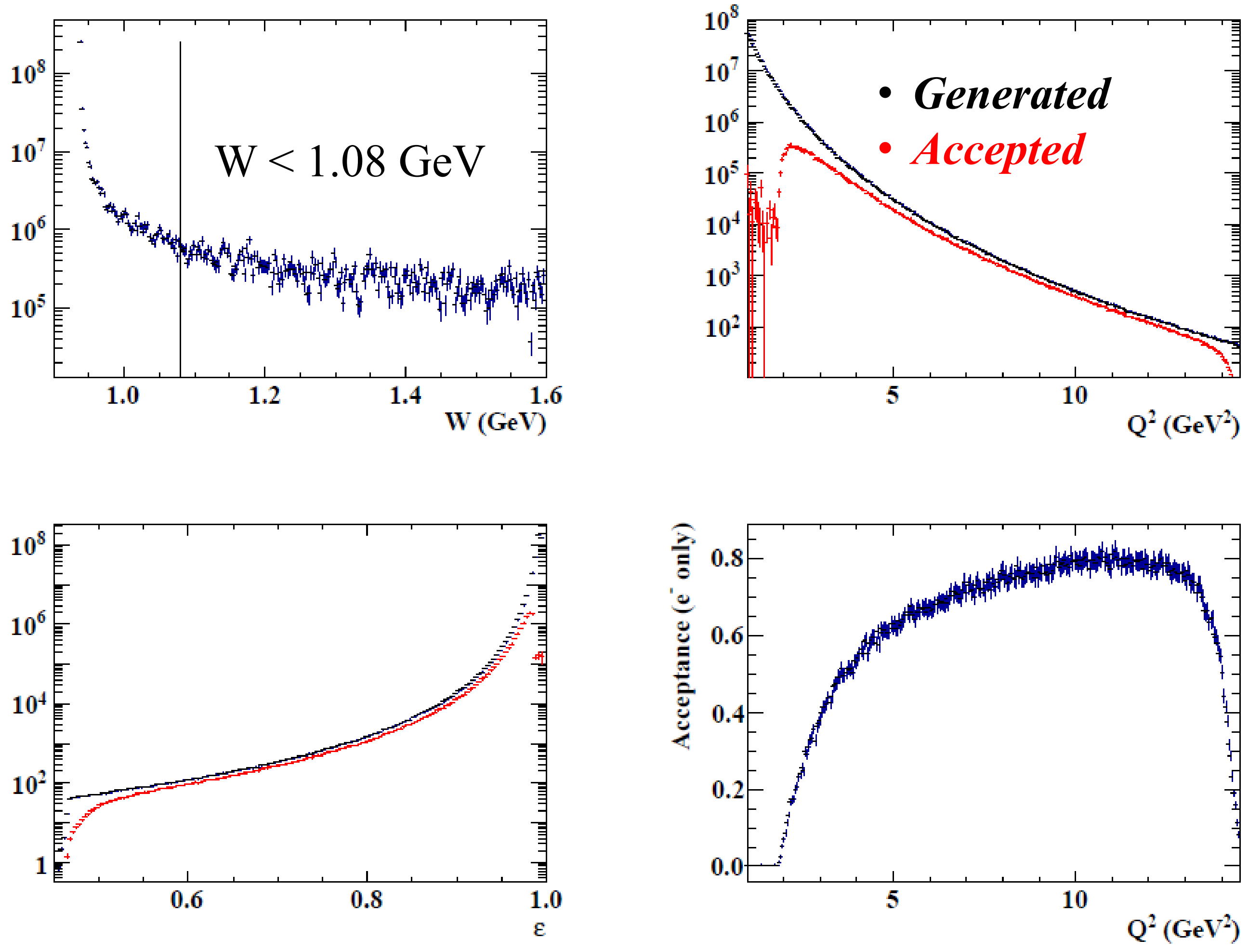

BigCal Radiation Damage

- Radiation Damage: relative gain vs. cumulative beam charge:
  - Energy resolution degraded from 10%/√E to ~21%/√E at end of experiment due to radiation damage
  - Coordinate resolution not strongly affected

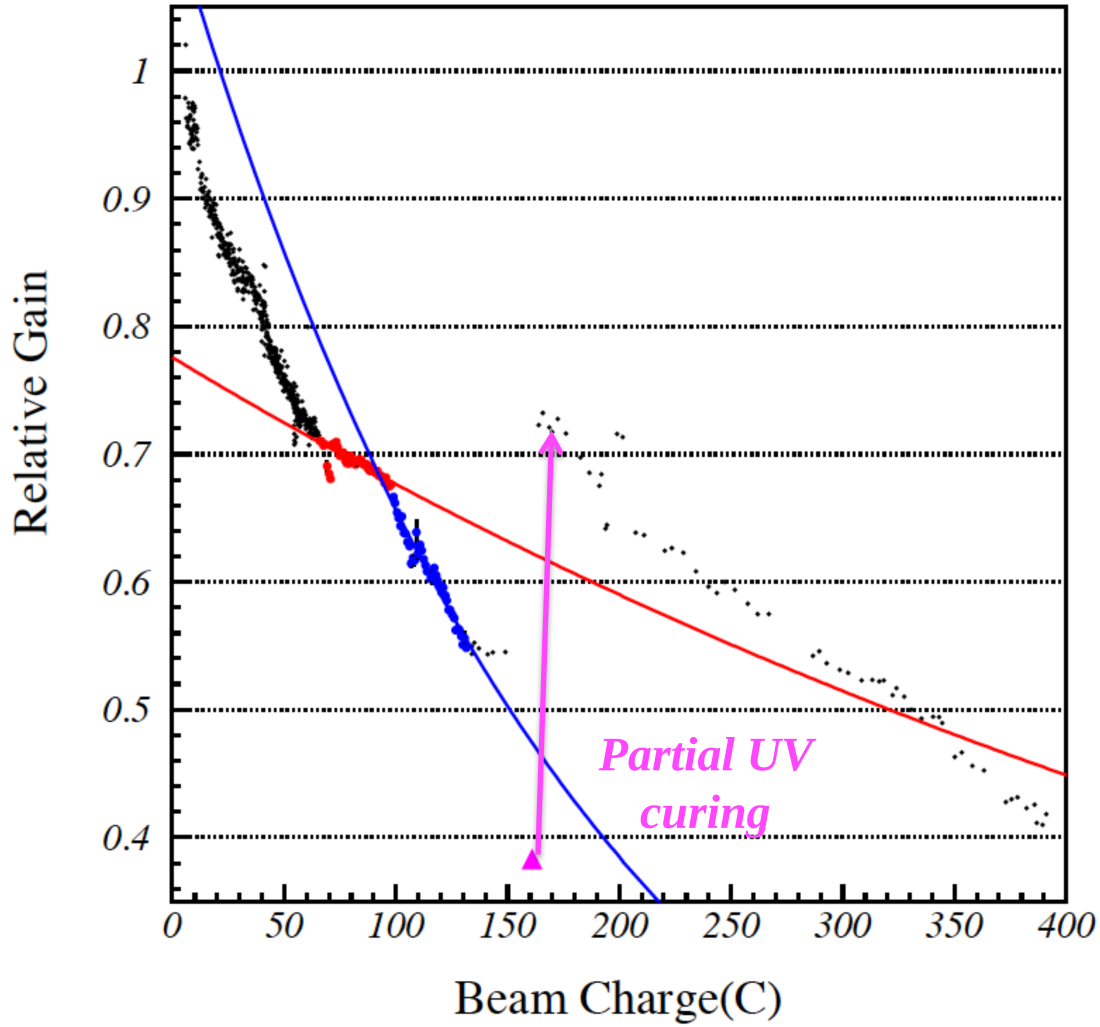

Maximum-likelihood Method

$$\mathcal{L}(P_t, P_\ell) = \prod_{i=1}^{N_{\rm event}} \frac{1}{2\pi}\{1 + \lambda_0(\varphi_i) + h_i P_e A_y^{(i)} \times [(S_{xt}^{(i)} P_t + S_{x\ell}^{(i)} P_\ell)\cos\varphi_i - (S_{yt}^{(i)} P_t + S_{y\ell}^{(i)} P_\ell)\sin\varphi_i]\},$$

$$\lambda_t^{(i)} \equiv h_i P_e A_y^{(i)} (S_{xt}^{(i)} \cos\varphi_i - S_{yt}^{(i)} \sin\varphi_i),$$
$$\lambda_\ell^{(i)} \equiv h_i P_e A_y^{(i)} (S_{x\ell}^{(i)} \cos\varphi_i - S_{y\ell}^{(i)} \sin\varphi_i).$$

$$\sum_{i=1}^{N_{event}} \begin{pmatrix} \left(\lambda_t^{(i)}\right)^2 & \lambda_t^{(i)}\lambda_\ell^{(i)} \\ \lambda_t^{(i)}\lambda_\ell^{(i)} & \left(\lambda_\ell^{(i)}\right)^2 \end{pmatrix} \begin{pmatrix} P_t \\ P_\ell \end{pmatrix} = \sum_{i=1}^{N_{event}} \begin{pmatrix} \lambda_t^{(i)}\left(1-\lambda_0^{(i)}\right) \\ \lambda_\ell^{(i)}\left(1-\lambda_0^{(i)}\right) \end{pmatrix}$$

- P_T, P_L are extracted using an unbinned maximum likelihood method, which reduces to a system of linear equations for small asymmetries, as typically observed in this experiment.
- Beam polarization and analyzing power appear in estimators for P_T, P_L, but cancel in the ratio P_T/P_L
- Accounts for spin precession in a straightforward way

GEp-2γ: See C. F. Perdrisat for more details

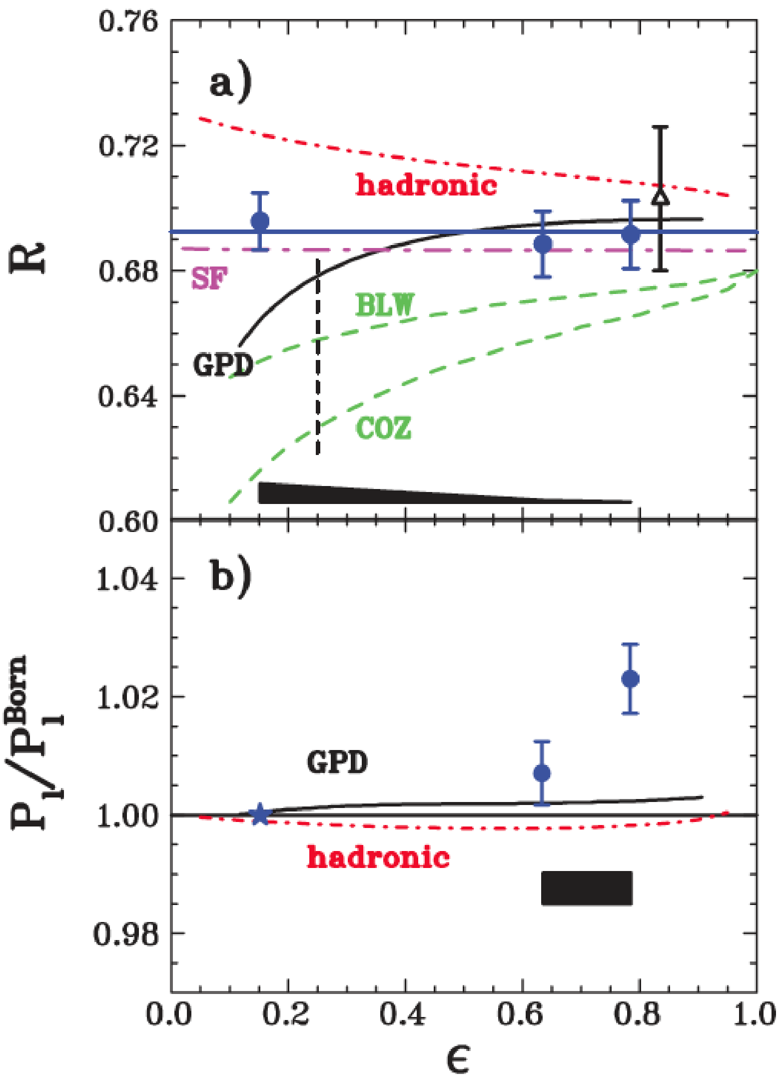

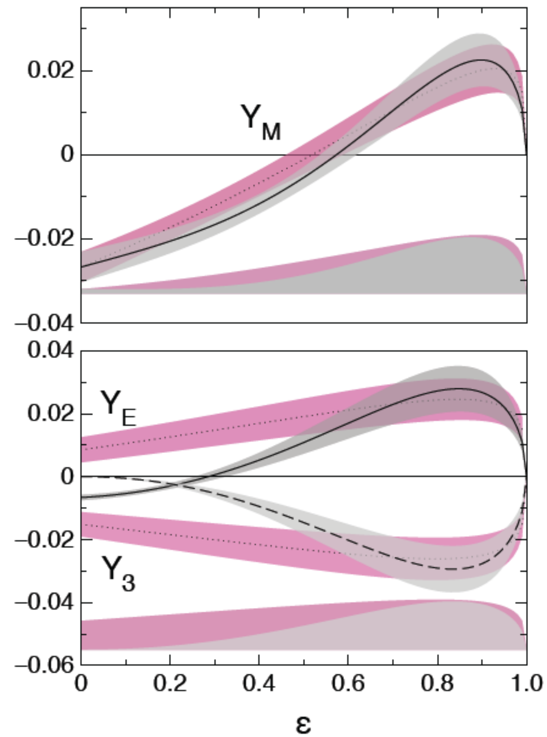

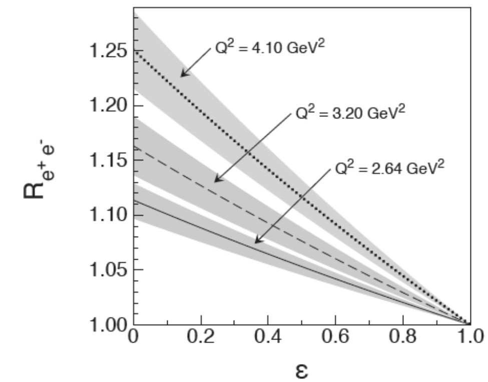

Determination of two-photon-exchange amplitudes from elastic electron-proton scattering data: arxiv:1012.0564

$$T_{h,\lambda'_N\lambda_N} = (e^2/Q^2)\,\bar{u}(k',h)\gamma_\mu u(k,h) \times \bar{u}(p',\lambda'_N)\left(\tilde{G}_M\,\gamma^\mu - \tilde{F}_2\frac{P^\mu}{M} + \tilde{F}_3\frac{\gamma\cdot K P^\mu}{M^2}\right)u(p,\lambda_N),$$

$$Y_M \equiv \mathcal{R}\left(\delta\tilde{G}_M/G_M\right), \quad Y_E \equiv \mathcal{R}\left(\delta\tilde{G}_E/G_M\right),$$

$$Y_3 \equiv \left(\nu/M^2\right)\mathcal{R}\left(\tilde{F}_3/G_M\right).$$